AD-A132 177 NUCLEATION AT A LIQUID-LIQUID INTERFACE AND EXPLODING DROPS IN EMULSIFIED FUEL COMBUSTION(U) PRINCETON UNIV N J DEPT OF AEROSPACE AND MECHANICAL SCIENCES. 1/2

UNCLASSIFIED C T AVEDISIAN JUL 76 PUAMS-1315 F/G 21/2 NL

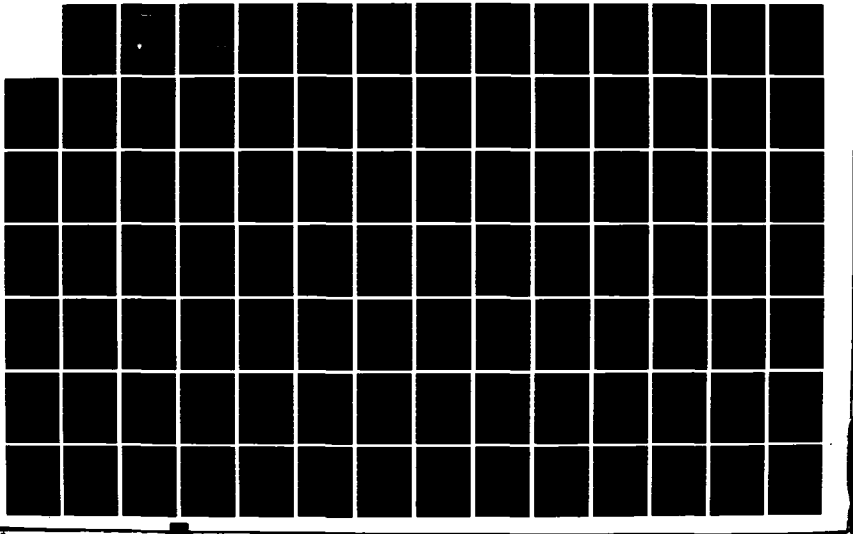

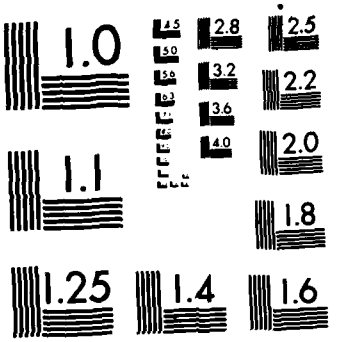

MICROCOPY RESOLUTION TEST CHART
NATIONAL BUREAU OF STANDARDS-1963-A

09

Princeton University

Nucleation at a Liquid-Liquid Interface and Exploding Drops in Emulsified Fuel Combustion

C.T. Avedisian

Aerospace and Mechanical Sciences Report #1315

July, 1976

Department of Aerospace and Mechanical Sciences

(1)

Nucleation at a Liquid-Liquid Interface and Exploding Drops in Emulsified Fuel Combustion

C.T. Avedisian

AMS

Aerospace and Mechanical Sciences Report #1315

July, 1976

School of Engineering and Applied Science

Princeton University

Princeton, New Jersey 08540

Introduction

This progress report gives some preliminary observations of the exploding drop phenomenon which sometimes occurs during burning of emulsified fuels. It contains what may be considered a first attempt at explaining the so-called "micro-explosion" effect which has been observed in the burning of such fuels.

The purpose of this work was twofold: 1) to offer an explanation for the droplet explosion effect and thereby predict the temperature at which an emulsified fuel drop would explode; and 2) to report the results of an experimental attempt to measure this maximum or explosion temperature.

The model for the explosion phenomenon is based on the assumption that boiling at the internal phase-fuel interface in the emulsion is responsible for droplet break-up. An expression for the rate at which bubbles form homogeneously at the interface is presented and used to predict the corresponding nucleation temperature. This expression is a very simplified form of a description of nucleation in systems of more than one active species. The assumption is basically that the flow of nuclei past the critical size is independent of the molecular species causing the transition. This assumption is probably valid only for nuclei which are already so near to the critical size that they have substantially reached their equilibrium composition. A more accurate treatment would have to take into account the shape of the free energy surface to predict the rate of flow of nuclei through the corresponding saddle point. The results for these two cases should not be expected to differ too greatly because the energy of forming the critical nucleus is the

same for both cases.

The experimental method consisted of injecting a drop of the test emulsion in the bottom of a column filled with a heavier immiscible liquid under a temperature gradient. The rising droplet is progressively heated until a temperature is reached at which point the droplet suddenly explodes. This configuration models combustion of a single fuel drop in that the droplet surface temperature from the point of ignition to steady state burning increases. The steady state droplet burning temperature is limited by the boiling point of the fuel. However, in the experiment described here the emulsion drop can be heated to a temperature as high as 90% of the critical temperature of the fuel. The advantages of this are obvious when one considers that for some fuel emulsions the predicted nucleation temperature is higher than the boiling point of the fuel.

Four water-pure fuel emulsions were tested: 1) water-decane; 2) water-dodecane; 3) water-tetradecane; and 4) water-hexadecane. The predicted and measured nucleation temperatures are in remarkably good agreement (that is, with the highest measured temperatures). The results indicate that for free droplet burning at 1 atmosphere pressure only the water-hexadecane emulsion should burn explosively.

It must be finally pointed out that it is implicitely assumed in this work that an emulsion can indeed exist in the superheated state as a fuel drop containing relatively immobile water microdroplets, and that these water drops are in fact immiscible in the fuel even at high temperatures. This assumption has not yet been rigorously tested, but it is so basic to any work concerning the

burning of emulsified fuels (by definition) that it is for the present accepted.

The period of this work was approximately from September 1975 to July 1976 and formed part of a program generally concerned with the burning characteristics of emulsified fuels in the Guggenheim Laboratories at Princeton University.

Table of Contents

I. Kinetics of Nucleation at a Liquid-Liquid Interface

1. Nucleation Rate and Equilibrium Number of Nuclei

The spontaneous formation of tiny vapor nuclei in bulk liquid is a random event. Density fluctuations in the liquid create cavities or voids which act as sites for the vaporization of single molecules. These molecules randomly collide with or escape from a vapor cavity and increase or decrease its size by a proportional amount. Growth occurs by single vapor molecules being absorbed on the surface of the bubble one at a time. The probability of simultaneous collisions of two or more molecules is very low and not considered.

Growth continues in this way until a certain size, known as the critical size, is reached. Further increasing the number of molecules in the bubble beyond this size leads to a rapid growth to macroscopic size, often observed as explosive vaporization. The critical size represents the dividing point between a stable liquid and a stable vapor phase. Right at the critical size the bubble is in a metastable state.

The kinetics of bubble growth up to the critical size is assumed to occur at a slow enough rate so that the principle of detailed balancing may be employed. Beyond the critical size growth is rapid and explosive boiling occurs. Growth beyond the critical size cannot therefore be described by this model. But this is perfectly acceptable because all bubbles which reach the critical size are considered to grow spontaneously to macroscopic size. The problem therefore ends at the point where the theory does not apply.

It is sufficient to have just one nucleus in a given volume reach the critical size for explosive boiling to occur. When this happens in an emulsified fuel, the primary droplet may be completely shattered by the rapid growth of the nucleus to macroscopic size. In the general case the number of nuclei which grow to critical size is usually termed the nucleation rate, J, in units of nuclei formed/cm^3-sec. The nucleation rate depends very strongly on temperature, as expected, and is negligible for all but a very narrow temperature range. This range determines the temperature of explosive boiling.

These ideas have been utilized extensively in the literature to determine the nucleation rate for boiling in the bulk of a liquid - homogeneous nucleation. Nucleation at a liquid-liquid interface requires only a physically based extension of current theories.

Consider fig. 1. A vapor bubble has formed at the interface between liquids a and b. Unlike homogeneous nucleation, as for example in the bulk of liquid a, both a and b molecules have access to the nucleus. The nucleus can grow or decay by molecular interchange with either a or b molecules. It is assumed that molecules of a cannot penetrate the interface and enter liquid b (vice versa for b molecules). This is not strictly correct because the interface is really a region in which the liquids are mutually saturated. Nevertheless this so-called "rigid plane" model of the interface between two liquids leads to results which are consistent with experimental measurements and so will be adopted here.

With this understanding of the interface it is seen that b molecules can only enter the nucleus by colliding with that part of the nucleus surface lying on the b side (the heavy dark surface shown in fig. 1), and a molecules can only be absorbed into the nucleus by collisions with the surface of the nucleus lying on the a side. These surfaces are called the transfer area for b molecules, S_b, and the transfer area for a molecules, S_a, respectively.

Performing an analysis similar to that presented in reference 3 but now accounting for bubble growth by molecular absorption on more than one transfer area (there is only one transfer area in homogeneous nucleation), the rate of formation of nuclei per unit volume and time which grow to the critical size is

$$J = \frac{\Sigma[S_i(x)\beta_i]}{\int_1^\infty \frac{dx}{n(x)}} \qquad 1$$

where the summation extends over molecules of kind i which have access to the nucleus through transfer area S_i.

β_i is the rate at which molecules of kind i strike and are absorbed on transfer area $S_i(x)$. For spherical and perfectly elastic ideal gas molecules the number of i molecule collisions per unit of transfer area and time is

$$\beta_i = \frac{P_i''}{\sqrt{2\pi m_i kT}} \qquad 2.$$

m_i is the molecular mass, P_i'' is the partial pressure of species i.

at the external liquid pressure, k is the Boltzmann constant, and T is temperature. Equation 2 accounts for the basic growth mechanism in nucleation theory - random molecular collisions on the surface of the nucleus.

n(x) is the number of nuclei containing x molecules in a unit volume when J = 0 where

$$x = \Sigma x_i \qquad 3.$$

It may be assumed outright as a Boltzmann distribution (ref. 4). Alternatively the system of nuclei and liquid molecules can be modelled as an ideal dilute solution and the free energy of mixing minimized. In either case the result is the same:

$$n(x) = N \exp(-W(x)/kT) \qquad 4$$

where W(x) is the thermodynamical work of forming a vapor nucleus containing x molecules, and N is the number of liquid molecules in a unit volume with which the n(x) nuclei are "mixed" to form this hypothetical solution.

The limits of integration in equation 1 extend over nuclei containing from 1 to an infinite number of vapor molecules (a single vapor molecule is viewed as the smallest nucleus). This boundary condition arises from the assumption that there are no nuclei containing $x \gg x_{crit}$ molecules. It is mathematically convenient to take this number as infinity. This and other approximations used in homogeneous nucleation theory are discussed in reference 2. It is assumed here that these same approximations apply to nucleation at a liquid-liquid interface.

The value of N in equation 4 depends on the location of bubble formation. For nucleation inside a liquid drop of radius r containing liquid a, the number of molecules in the drop is

$$N_a = (r/r_a)^3 \qquad 5a$$

where r_a is the radius of the assumed hard sphere molecule. Eq. 5a assumes that the total droplet volume is the sum of e hard sphere molecular volumes of the molecules inside the . uid drop. Similarly the number density of a molecules on droplet surface

$$N_{as} = (r/r_a)^2 \qquad 5b.$$

Equation 5b assumes that the total surface area of a liquid drop of radius r is the sum of the surface areas of the hard sphere molecules of radius r_a. Combining equations 5a and 5b, the number of a molecules on the surface of the drop is

$$N_{as} = N_a^{2/3} \qquad 6.$$

The interface between two liquids really consists of both a and b molecules. Fig. 2 shows a hypothetical illustration of such an interface. If the A-C region in fig. 2 defines the interface, the number of molecules in a unit volume at the interface will be the sum of the number densities of the a and b molecules so that

$$N = N_a^{2/3} + N_b^{2/3} \qquad 7.$$

(The number density of b molecules is referred to a droplet of

radius r containing only b molecules so that $N_{bs} = N_b^{2/3}$).

The equilibrium number density for homogeneous nucleation within liquid a can now be written as follows:

$$n(x) = N_a \exp(-W(x)/kT) \qquad 8.$$

For nucleation at the interface between liquids a and b, equation 7 substituted into equation 4 gives

$$n(x) = (N_a^{2/3} + N_b^{2/3}) \exp(-W(x)/kT) \qquad 9.$$

The work terms in equations 8 and 9 are not the same because the geometry of bubble growth in the bulk of a liquid is different from that at the interface. The difference is primarily that of a spherical nucleus (homogeneous nucleation) and a lens shaped bubble (nucleation at the interface between the two liquids).

For nucleation in bulk liquid, $N^{2/3} \rightarrow N$ as one must now consider the hypothetical nuclei-liquid molecule solution as made up of the bulk liquid molecules and vapor nuclei with each liquid molecule within the drop being viewed as a potential bubble. This modification is further discussed in reference 5.

For nucleation at the interface between two liquids equation 1 becomes

$$J = [S_a(x)\beta_a + S_b(x)\beta_b] \frac{1}{\int_1^\infty \frac{dx}{n(x)}} \qquad 10.$$

This equation has the form $J = J_a + J_b$ where J_a is the number of nuclei formed as a result of growth by absorption of only a molecules on transfer area S_a (J_b is similarly defined).

Combining equations 2, 4, and 10 gives the nucleation rate at the interface between two liquids:

$$J = \frac{N}{(2\pi kT)^{\frac{1}{2}}}\left[\frac{P''_a S_a(x)}{m_a^{\frac{1}{2}}} + \frac{P''_b S_b(x)}{m_b^{\frac{1}{2}}}\right] \frac{1}{\int_1^\infty \frac{dx}{\exp(-W(x)/kT)}} \qquad 11$$

where

$$N = N_a^{2/3} + N_b^{2/3} \qquad 7$$

and

$$x = x_a + x_b \qquad 3.$$

2. Specific Location of Bubble Growth at the Interface

To determine the nucleation rate from equation 11 it is necessary to know the work of formation of a vapor nucleus containing x total molecules. This work should obviously depend on the geometry and particular location of bubble growth. For a droplet of liquid a in liquid b a vapor nucleus can form at any of the following positions (see fig. 3):

1. completely within liquid a (homogeneous nucleation in liquid a - fig. 3a);
2. at the interface between liquids a and b but entirely surrounded by liquid a except possibly for an opening large enough to permit b molecules to enter -

fig. 3b;

3. between liquids a and b and actually separating the interface. The bubble can be considered as two spherical caps joined together - a lens (fig. 3c);
4. at the interface and entirely surrounded by liquid b except for an opening just large enough to permit a molecules to enter the bubble (fig. 3d); and
5. completely within liquid b (homogeneous nucleation in liquid b - fig. 3e).

When liquid a is more volatile than liquid b it is necessary to introduce the concept of a bubble completely surrounded by liquid b except for an opening just large enough to permit a molecules to enter. Without this artifice a bubble forming in this way will contain only b molecules so that the energy of bubble formation will be the same as for homogenous nucleation in liquid b. If the temperature in liquid b is unable to reach its corresponding superheat temperature, explosive vaporization will not occur. This will certainly be the case in emulsified fuel combustion because the steady-state burning temperature does not even reach the fuel (liquid b) boiling point let alone become superheated. Yet in the experiments to be reported the bubble growth geometry was predicted to be the same as that shown in fig. 3d and nucleation was still observed to occur even though the corresponding temperature was far below the limit of superheat of the fuel. This apparent anomaly can best be explained by assuming that both a and b molecules are in the bubble so that the

bubble gas pressure is the sum of the partial pressures of a and b; $P'' = P''_a + P''_b$. It will later be shown that the solution of equation 11 can be put in the form

$$T \sim \sigma^3/(P'' - P_o)^2$$

where P_o is the ambient liquid pressure and σ is surface tension. From this approximate proportionality it is seen that an increase in the gas pressure lowers the expected temperature of nucleation at constant P_o and σ. In the experiments which formed a part of this program, the a and b liquids were such that $P''_a >> P''_b$ so that the increase in P" on including molecules of a in the nucleus was substantial. This increase in total gas pressure is apparently just enough to bring theory and experiment into good agreement. Some means must be provided to enable molecules of a to enter a bubble formed "entirely" in liquid b, and the concept of a transfer area of molecular dimensions is introduced. No modification of the theory leading to eq. 11 is necessary to account for a molecules in the nucleus. $S_a(x)$ just becomes proportional to the molecular surface area of an a molecule .

When a nucleus is predicted to form in liquid b away from the interface (fig. 3e) and $P''_a >> P''_b$, molecular diffusion of a molecules through liquid b must be included in the theory which is based on bubble formation due to random molecular motion. The only thing which would be effected if this were done would be the pre-exponential term in the solution of eq. 11 .

These arguemnts lead to the conclusion that when one liquid is

much more vo atile than the other and homogeneous nucleation in the less volatile liquid is predicted to occur, the corresponding temperature is closer to what would be expected for nucleus formation at the interface - fig. 3d. Exactly how much more volatile one liquid must be than the other for this to be true is unknown at this time. The experimental results reported here suggest that a one order of magnitude difference in vapor pressure satisfies this condition.

When a bubble forms entirely in liquid a as shown in fig. 3b, the above arguments apply if $P''_b >> P''_a$. Otherwise if $P''_a >> P''_b$ they are superfluous. Even if molecules of b are in the bubble, the much greater volatility of liquid a implies that the gas pressure is almost entirely due to the partial pressure of a. The only difference between bubble formation as shown in figs. 3a and 3b is that one must now consider liquid molecules at the interface and not liquid molecules in the bulk of liquid a (fig. 3a) as potential nuclei. The pre-exponential factor in the expression for the nucleation rate is thus reduced by about 10^6 $(N \rightarrow N^{2/3})$.

It is now apparent that one needs to know both the location and work of formation of a nucleus to be able to solve eq. 11 because W(x) will be slightly different for the various positions of bubble growth shown in fig. 3. For this purpose it would be useful to prescribe conditions which could be used to estimate the position of bubble formation. Such conditions, if based on the physical properties of the two liquids, would provide a

powerful prediction tool for nucleation at a liquid-liquid interface. These criteria can be determined by first considering the energy to form a bubble separating the interface between liquids a and b (fig. 3c). From this geometry the limiting case of a completely spherical nucleus and corresponding conditions for its attainment can be determined.

II. Thermodynamics of Bubble Growth at a Liquid-Liquid Interface

1. Basic Assumptions

Bubble growth at a liquid-liquid interface is assumed to occur under the following conditions:

1. Bubble growth up to the critical size occurs reversibly so that it is at all times in mechanical equilibrium;
2. The temperature is constant;
3. The external liquid pressure is constant;
4. The total volume of nucleus and surrounding liquid is constant (closed system);
5. The characteristic nucleus dimension (e.g., radius) is much smaller than the radius of curvature of the interface at which the bubble grows;
6. Bulk liquid and vapor properties can be used to describe the thermodynamic state of the bubble;
7. The vapor in the bubble is an ideal solution of ideal gases;
8. The two liquids on either side of the interface are completely immiscible; and
9. One liquid is much more volatile than the other so that $P''_a >> P''_b$ (a denotes the volatile liquid).

The first assumption implies that Laplace's equation can

be used to relate the gas pressure to the bubble radius. This has been critized in reference 6 because no account is taken of viscosity and inertia forces during bubble growth to the critical size. The equation of motion of bubble growth should really be solved to determine the relation between the bubble gas pressure and bubble radius. This, however, greatly complicates the solution and would in any case have a small effect on the nucleation temperature because such non-equilibrium effects would appear only in the pre-exponential term in the solution of eq. 11.

The second assumption arises from the fact that the nucleation rate is negligible until a temperature range is reached at which the rate becomes very large - the temperature range of expected nucleation. This temperature range is typically within 1C to 2C of the limit of superheat for homogeneous nucleation and should also be representative of nucleation at a liquid-liquid interface. The entire event of bubble growth to macroscopic size can therefore be considered to begin and end (growth to macroscopic size) at a temperature which is within about 2C of the actual superheat temperature.

A hypothetical system is constructed consisting of a single bubble and surrounding liquid bounded by a control surface across which no mass flows (fig. 4b). Bubble growth proceeds by vaporization of the liquid molecules within this closed system. The total number of molecules is therefore the same before and after the appearance of the nucleus (figs. 4a and 4b).

In emulsified fuels the internal phase diameter can be as

small as 10^{-4} cm. However, because a nucleus of critical size is typically 10^{-7} cm in diameter droplet curvature may therefore be neglected ($10^{-4} >> 10^{-7}$).

The use of bulk liquid properties to describe the state of a microscopic bubble was studied in reference 7. It was concluded that because the effect of bubble curvature on surface tension cannot be accurately estimated, it is a good first approximation to use the bulk liquid surface tension in describing the state of the critical nucleus. The experiments reported here and in the literature indicate that this is an excellent assumption.

The effect of vapor non-ideality in homogeneous nucleation was examined in reference 8. It was concluded that for boiling in pure liquids this effect is very small.

In addition to being satisfied for the particular a and b liquids used here, the last assumption provides a mathematical convenience which enables eq. 11 to be integrated. Without this assumption an analytical solution to eq. 11 cannot be obtained.

The reversible work of forming a nucleus at a liquid-liquid interface can now be determined using the above assumptions. For this purpose the following section reviews those aspects of thermodynamics which are important to this problem.

2. Thermodynamics of Nucleation

The first law of thermodynamics for a reversible process is

$$dU = dQ_{rev} - \Sigma\, dW_{rev} \qquad 12$$

where ΣdW_{rev} represents all forms of reversible work which the system can exchange with its surroundings, dU is the change of accumulated energy of the system, and dQ represents the exchange of heat between the system and its surroundings. For bubble growth at a liquid-liquid interface ΣdW_{rev} includes contributions from expansion, surface, and chemical work so that the total work is

$$\Sigma dW_{rev} = \Sigma P_k dV_k - \Sigma u_i dx_i - \Sigma \sigma_j dA_j \qquad 13.$$

u_i and x_i are the chemical potential and number of molecules of species i respectively.

The first term in eq. 13 represents the expansion work contribution to the total work of a system which is divided into k subsystems each of volume V_k and pressure P_k. If for example one of these subsystems consists of a vapor volume containing two species then $P_k = \Sigma P_i = P''_a + P''_b$. Writing the expansion work term in the form shown in eq. 13 is convenient, though somewhat unusual, for studying the thermodynamics of the nucleation process.

The summation in the second term in eq. 13 extends over the number of different species in each phase present in the total system. The energy required to create or destroy surfaces within the total system is represented by the last term in eq. 13 where σ_j is the surface tension of the A_j surface. The summation extends over the number of surfaces in the system. These surfaces include bubble surfaces and interfacial areas between liquids (in

which case σ_j is the interfacial tension between the two liquids).

The second law of thermodynamics for a reversible process is

$$dQ_{rev} = TdS \qquad 14.$$

The combination of equations 12,13, and 14 gives the total internal energy in each differential piece of matter:

$$dU = TdS - \Sigma P_k dV_k + \Sigma u_i dx_i + \Sigma \sigma_j dA_j \qquad 15.$$

When the system for which eq. 15 is valid undergoes a change in <u>size</u> only, the extensive properties S, V, x, and A will change by a proportional amount. The amount of these changes is such that the intensive properties T, P_k, u_i, and σ_j do not change. Under these conditions integration of eq. 15 between the initial and final states of this hypothetical size change gives

$$\Delta U = T\Delta S - \Sigma P_k \Delta V_k + \Sigma u_i \Delta x_i + \Sigma \sigma_j \Delta A_j .$$

Only the size of the system has been increased so that the final state must be some multiple of the initial state. Since the extensive properties depend only on size, they all change by the same amount. Therefore from the above equation,

$$U = TS - \Sigma P_k V_k + \Sigma u_i x_i + \Sigma \sigma_j A_j \qquad 16.$$

Equation 16 gives the internal energy of a system of <u>finite</u> size.

The differential of equation 16 is

$$dU = TdS + SdT - \Sigma P_k dV_k - \Sigma V_k dP_k + \Sigma u_i dx_i + \Sigma x_i du_i + \Sigma \sigma_j dA_j + \Sigma A_j d\sigma_j$$

This equation must still satisfy equation 15. This implies that eq. 17 below must be valid:

$$SdT - \Sigma V_k dP_k + \Sigma x_i du_i + \Sigma A_j d\sigma_j = 0 \qquad 17.$$

Eq. 17 is a form of the Gibbs-Duhem equation. For bubble growth at constant temperature, $dT = 0$ and $d\sigma_j \approx 0$ since σ_j is a strong function of temperature and may only very weakly depend on pressure. Eq. 17 then becomes

$$\Sigma V_k dP_k = \Sigma x_i du_i \qquad 18.$$

Assuming each liquid and vapor species is confined to only one sub-system volume, the subscript "k" in eq. 18 can be replaced by the subscript "i" so that

$$\Sigma V_i dP_i = \Sigma x_i du_i.$$

If, for example, the ith species is a vapor contained in a volume V_i, then P_i would be its corresponding partial pressure. Under the condition stated above, this particular species in the vapor phase will not be present in any other sub-system volume.

It is now assumed that for the above equation to be satisfied each term on the left hand side must be equal to the term corresponding to the same species and phase on the right hand side. If this is a valid assumption, one can write

$$V_i dP_i = x_i du_i \qquad 19.$$

Equation 19 relates the chemical potential of the ith species

in the liquid (') or vapor (") phase to the volume in which it is contained at corresponding pressure P_i. For an ideal gas,

$$P_i'' V_i'' = x_i'' kT$$

so that eq. 19 becomes

$$kT \frac{dP_i''}{P_i''} = du_i''$$

Integrating the above equation between some arbitrary sub-critical vapor pressure, P_i'', and the vapor pressure in the critical size bubble, P_{ic}'', gives

$$u_i''(P_i'',T) - u_{ic}''(P_{ic}'',T) = kT \ln(P_i''/P_{ic}'') \qquad 20a.$$

A nucleus at the critical size is in chemical equilibrium so that the vapor chemical potential of species i is equal to its liquid chemical potential:

$$u_{ic}''(P_{ic}'',T) = u_i'(P_i',T).$$

Combining the above condition with eq. 20a relates the chemical potential of liquid and vapor in a nucleus of sub-critical size:

$$u_i''(P_i'',T) - u_i'(P_i',T) = kT \ln(P_i''/P_{ic}'') \qquad 20b.$$

Equations 16 and 20b will be particularly useful in determining the energy of formation of a bubble at a liquid-liquid interface. For this purpose it is convenient to use the Helmholtz function because the minimum work in a constant temperature pro-

cess is equal to the decrease of the Helmholtz function for the system.

The Helmholtz free energy is defined as

$$F = U - TS \qquad 21.$$

The differential of equation 21 is the following:

$$dF = dU - TdS - SdT \qquad 22.$$

Substituting equations 12 and 14 into eq. 22 gives,

$$dF = - \Sigma\, dW_{rev} \qquad 23.$$

The Helmholtz free energy is therefore minus the total work obtainable from an isothermal process.

Equations 16 and 21 give the Helmholtz free energy of a system of finite size:

$$F = - \Sigma\, P_k V_k + \Sigma\, u_i x_i + \Sigma\, \sigma_j A_j \qquad 24.$$

This is the basic equation used to determine the free energy of bubble formation. To do this, two systems of finite size are considered, one with and the other without a nucleus. The change in free energy between the two systems as determined by eq. 24 applied to each gives the minimum work of forming a bubble of specified size.

3. Work of Bubble Formation at a Liquid-Liquid Interface

Consider the total system shown in fig. 4a bounded by a control volume (dotted line). The total system consists of two pure liquid sub-systems which are separated by an interface

(modelled as essentially a dividing line between the two liquids). The total system consists of x'_{a1} molecules of liquid a at a liquid pressure P'_{a1}, volume V'_{a1}, and liquid chemical potential u'_{a1} (similarly for liquid b).

After the appearance of a single bubble at the interface, the total system consists of three sub-systems as shown in fig. 4b. The total system boundary is the same as in fig. 4a so that the total volume has not changed. The presence of the bubble implies, however, that the sub-system volumes must have changed. The temperature is the same before and after the appearance of the bubble.

The Helmholtz free energy of the system without the bubble (fig. 4a) is the following:

$$F_a = x'_{a1}u'_{a1} + x'_{b1}u'_{b1} + \sigma_{ab}S_{ab1} - P'_{a1}V'_{a1} - P'_{b1}V'_{b1} \qquad 25.$$

Similarly for the system in fig. 4b the free energy as determined from eq. 24 is,

$$F_b = x'_{a2}u'_{a2} + x'_{b2}u'_{b2} - P'_{a2}V'_{a2} - P'_{b2}V'_{b2} + \sigma_{ab}S_{ab2} + (x''_b u''_b + x''_a u''_a - P''V''_b + \sigma_a S_a + \sigma_b S_b) \qquad 26.$$

The quantity in brackets in eq. 26 represents the energy contribution from the bubble at the interface. The important point to note in eq. 26 is that the presence of both a and b molecules in the bubble has been accounted for by including the chemical energy of b molecules in the bubble, $x''_b u''_b$. This is consistent with the assumption that bubble growth occurs by molecular

absorption on the appropriate transfer areas, S_a or S_b so that $P'' = P''_a + P''_b$ in eq. 26.

Including terms such as $\sigma_a \Delta_a$ or $\sigma_b \Delta_b$ in eq. 26, as for example one might be tempted to do to determine the energy of bubble formation for growth as shown in figs. 3b and 3d, will always be negligible compared to either $\sigma_a S_a$ or $\sigma_b S_b$ except possibly for conditions which would be of no practical interest.

The following relations apply as a consequence of the previously mentioned assumptions:

$$x'_{a1} = x'_{a2} + x''_a \qquad 27;$$

$$x'_{b1} = x'_{b2} + x''_b \qquad 28;$$

$$V'_{a1} + V'_{b1} - (V'_{a2} + V'_{b2}) = V''_b \qquad 29.$$

The number of a and b vapor molecules is assumed to be small compared to the number of a and b liquid molecules respectively. With constant a and b liquid pressures (assumption 3 on page 11), the liquid chemical potentials in the two systems shown in figs. 4a and 4b will be the same:

$$u'_{a1} \approx u'_{a2} \qquad 30;$$

$$u'_{b1} \approx u'_{b2} \qquad 31.$$

In the specific application of the results of this investigation, liquid a is dispersed as small drops in a larger mass of liquid b. There will be a finite curvature of the interface between a and b (see fig. 5). Because the drop of liquid a is in mechanical equilibrium, the pressure across the interface is

given by the Laplace equation:

$$P'_{a1} - P'_{b1} = 2\sigma_{ab}/r_{ab} \qquad 32$$

where σ_{ab} and r_{ab} are liquid interfacial tension and liquid droplet radius respectively. For conditions of present interest $2\sigma_{ab}/r_{ab}$ is much less than either P'_{a1} or P'_{b1}. The pressure in the drop and surrounding liquid are therefore approximately the same (assumption 3):

$$P'_{a1} \approx P'_{b1}$$

$$P'_{a2} \approx P'_{b2}.$$

For bubble growth at constant liquid pressure it follows that $P'_{a1} \approx P'_{b1} \approx P'_{a2} \approx P'_{b2} = P_o$.

Subtracting eq. 26 from eq. 25 gives the total system free energy change on bubble formation:

$$\begin{aligned} F_a - F_b = {} & x'_{a1}u'_{a1} + x'_{b1}u'_{b1} + \sigma_{ab}S_{ab1} - P'_{a1}V'_{a1} - P'_{b1}V'_{b1} \\ & -x'_{a2}u'_{a2} - x'_{b2}u'_{b2} + P'_{a2}V'_{a2} + P'_{b2}V'_{b2} - \sigma_{ab}S_{ab2} \\ & -x''_{b}u''_{b} - x''_{a}u''_{a} + P''V''_{b} - \sigma_{a}S_{a} - \sigma_{b}S_{b} \end{aligned} \qquad 33.$$

Grouping terms and setting all liquid pressures equal to P_o, eq. 33 becomes,

$$\begin{aligned} F_a - F_b = {} & P''V''_{b} - P_o(V'_{a1} + V'_{b1} - V'_{a2} - V'_{b2}) - \sigma_{a}S_{a} - \sigma_{b}S_{b} \\ & - \sigma_{ab}(S_{ab2} - S_{ab1}) + x'_{a1}u'_{a1} + x'_{b1}u'_{b1} - x'_{a2}u'_{a2} \\ & - x'_{b2}u'_{b2} - x''_{b}u''_{b} - x''_{a}u''_{a} \end{aligned} \qquad 34.$$

Substituting equations 27 to 29 into eq. 34 and grouping terms gives the following:

$$F_a - F_b = V_b''(P'' - P_o) - \sigma_a S_a - \sigma_b S_b - \sigma_{ab}(S_{ab2} - S_{ab1}) - x_{b2}'(u_{b2}' - u_{b1}') - x_{a2}'(u_{a2}' - u_{a1}') - x_b''(u_b'' - u_{b1}') - x_a''(u_a'' - u_{a1}') \quad 35.$$

With equations 30 and 31, eq. 35 becomes

$$F_a - F_b = V_b''(P'' - P_o) - \sigma_a S_a - \sigma_{ab}(S_{ab2} - S_{ab1}) - x_b''(u_b'' - u_{b1}') - x_a''(u_a'' - u_{a1}') \quad 36.$$

The interfacial area between liquids a and b destroyed in forming the vapor bubble (fig. 4b) is related to S_{ab2} and S_{ab1} simply as $S_i = S_{ab1} - S_{ab2}$. Eq. 36 can then be re-written as

$$F_a - F_b = V_b''(P'' - P_o) - \sigma_a S_a - \sigma_b S_b + \sigma_{ab} S_i - x_b''(u_b'' - u_{b1}') - x_a''(u_a'' - u_{a1}') \quad 37.$$

From eq. 23 the minimum work required to form a vapor nucleus at the interface between two liquids is

$$W = x_b''(u_b'' - u_{b1}') + x_a''(u_a'' - u_{a1}') + V_b''(P_o - P'') + \sigma_a S_a + \sigma_b S_b - \sigma_{ab} S_i \quad 38.$$

The chemical potential differences in eq. 38 are related to the component partial pressures through eq. 20b so that eq. 38 can be

re-written as follows:

$$W = x_b'' kT \ln(P_b''/P_{bc}'') + x_a'' kT \ln(P_a''/P_{ac}'') + V_b''(P_o - P'') + \sigma_a S_a + \sigma_b S_b - \sigma_{ab} S_i \qquad 39.$$

The equation of state of an ideal gas can be used to eliminate x_a'' and x_b'' in eq. 39 (i.e., $x_b'' = P_b'' V_b''/kT$ and $x_a'' = P_a'' V_b''/kT$):

$$W = V_b''(P_b'' \ln(P_b''/P_{bc}'') + P_a'' \ln(P_a''/P_{ac}'') + P_o - P_a'' - P_b'') + \sigma_a S_a + \sigma_b S_b - \sigma_{ab} S_i \qquad 40.$$

where P'' in eq. 40 has been replaced by $P_a'' + P_b''$.

Eq. 40 is the final form of the work to form a vapor bubble at the interface between two liquids under the previously described assumptions. The first two terms in parenthesis represent chemical work, the third term is the work directed against pressure forces, the fourth and fifth terms represent the work to create the vapor surface areas S_a and S_b, and the last term is the work to destroy the liquid-liquid interfacial area S_i.

When liquid a is much more volatile than liquid b, $P_a'' >> P_b''$ and eq. 40 reduces to the expression given in reference 4.

For simplicity it is assumed that the nucleus shown in fig. 4b is a lens comprising two spherical caps joined together. With reference to fig. 6a, the bubble volume, V_b'', can be expressed in terms of r_a, r_b, and the contact angles θ and ϕ. From geometry the volumes of the two spherical segments shown in fig. 6a are,

$$v_a'' = 1/3\pi h_a^2(3r_a - h_a) = 1/3\pi r_a^3(3(h_a/r_a)^2 - (h_a/r_a)^3) \quad 41a,$$

and

$$v_b'' = 1/3\pi r_b^3(3(h_b/r_b)^2 - (h_b/r_b)^3) \quad 41b,$$

where

$$V_b'' = v_b'' + v_a'' \quad 41c.$$

Again from geometry,

$$M_a = \cos(\Psi) = (r_a - h_a)/r_a = 1 - h_a/r_a \quad 42a$$

and

$$M_b = \cos(\alpha) = 1 - h_b/r_b \quad 42b.$$

Combining equations 41 and 42 and rearranging terms, the total bubble volume is

$$V_b'' = 1/3\ \pi\ (r_b^3(2-3M_b+M_b^3) + r_a^3(2-3M_a+M_a^3)) \quad 43.$$

For the nucleus to be in mechanical equilibrium the forces at the edge of the lens must balance. A force balance at the bubble edge shown in fig. 6b results in the following expressions:

$$\sigma_{ab} - \sigma_a \cos(\theta) - \sigma_b \cos(\phi) = 0 \quad 44a;$$

and

$$\sigma_a \sin(\theta) - \sigma_b \sin(\phi) = 0 \quad 44b.$$

Combining equations 44 and and using the identity $\cos^2(\theta) + \sin^2(\theta) = 1$, one can also write the following:

$$\cos(\theta) = (\sigma_a^2+\sigma_{ab}^2-\sigma_b^2)/2\sigma_a\sigma_{ab} \quad 45a;$$

and

$$\cos(\phi) = (\sigma_b^2+\sigma_{ab}^2-\sigma_a^2)/2\sigma_b\sigma_{ab} \quad 45b.$$

Because the line of force of surface tension is tangent

to the spherical segment at the apex of the bubble and forms a right angle with the respective radii of curvature at that point, it follows that $\theta = \Psi$ and $\alpha = \phi$. Therefore, M_a and M_b can be expressed in terms of the surface and interfacial tensions by combining equations 42 and 45:

$$M_a = \cos(\theta) = (\sigma_a^2+\sigma_{ab}^2-\sigma_b^2)/2\sigma_a\sigma_{ab} \qquad 46a;$$

and

$$M_b = \cos(\phi) = (\sigma_b^2+\sigma_{ab}^2-\sigma_a^2)/2\sigma_b\sigma_{ab} \qquad 46b.$$

These expressions were derived in references 4 and 9. They hold theoretically only at the critical size, but a negligible error can be expected by applying them to nuclei which are "near" the critical size as mentioned previously.

The radii of curvature of the shperical caps, r_a and r_b, are related to each other as follows:

$$\sin(\alpha) = \sin(\phi) = \bar{a}/r_b;$$

and

$$\sin(\Psi) = \sin(\theta) = \bar{a}/r_a$$

where $\bar{a}$ is defined in fig. 6a and may be considered as the characteristic lens dimension. Combining the above two expressions provides a formula relating $\bar{a}$ to r_a and r_b:

$$\bar{a} = r_a\sin(\theta) = r_b\sin(\phi) \qquad 47.$$

Eliminating $\sin(\theta)$ and $\sin(\phi)$ between equations 47 and 44b gives the relation between radii of curvature and surface tension:

$$r_a/\sigma_a = r_b/\sigma_b \qquad 48.$$

The bubble volume can now be expressed in terms of either r_a or

r_b by substituting equation 48 into equation 43:

$$V_b'' = ((2-3M_a+M_a^3) + (2-3M_b+M_b^3)\sigma_b^3/\sigma_a^3)\pi r_a^3/3 \qquad 49a;$$

or alternatively

$$V_b'' = ((2-3M_b+M_b^3) + (2-3M_a+M_a^3)\sigma_a^3/\sigma_b^3)\pi r_b^3/3 \qquad 49b.$$

By defining

$$F = (\sigma_a^3(2-3M_a+M_a^3) + \sigma_b^3(2-3M_b+M_b^3))/4 \qquad 50a$$

and

$$F = \sigma_a^3 F_a = \sigma_b^3 F_b \qquad 50b,$$

the bubble volume becomes,

$$V_b'' = r_a^3 F_a \pi\, 4/3 = r_b^3 F_b \pi\, 4/3 \qquad 51.$$

F_a and F_b in equations 50 and 51 can now be considered as corrections applied to a spherical bubble of radius r_a or r_b so that its volume equals that of a lens whose surfaces have radii of curvature r_a and r_b. It should therefore be expected that for a spherical bubble of radius r_a, $F_a = 1$ (figs. 3a, 3b, 3d, and 3e). The conditions under which $F_a = 1$ and $F_b = 1$ will be shortly described.

The surface areas of the spherical caps are,

$$S_a = 4\pi r_a^2 A_a \qquad 52a,$$

and

$$S_b = 4\pi r_b^2 A_b \qquad 52b$$

where

$$A_a = (1-M_a)/2 \qquad 52c$$

and

$$A_b = (1-M_b)/2 \qquad 52d.$$

The liquid-liquid interfacial area destroyed by growth of the vapor lens of "radius" $\bar{a}$ is $S_i = \pi \bar{a}^2$. Combining this with equations 46a, 47, and the identity $\cos^2(\theta) + \sin^2(\theta) = 1$, the interfacial area becomes

$$S_i = \pi r_a^2 (1-M_a^2) \qquad 52e.$$

The work to form a bubble at the interface between two liquids can now be expressed as a function of r_a, P''_a, and P''_b by substituting equations 51 and 52 in eq. 40 and rearranging terms:

$$W = (P''_a \ln(P''_a/P''_{ac}) + P''_b \ln(P''_b/P''_{bc}) + P_o - P''_a - P''_b)\pi r_a^3 F_a 4/3 + 4\pi r_a^2 \sigma_a F_a \qquad 53.$$

At the critical size, $P''_a = P''_{ac}$ and $P''_b = P''_{bc}$ so that terms containing the natural logarithm in eq. 53 will vanish. If the bubble is near enough to the critical size for these terms to be very small compared to $P_o - P''_a - P''_b$ in eq. 53, it should be expected that a Taylor's series expansion of eq. 53 about conditions at the critical size will be a good approximation to the work of bubble formation. In addition the dominant contribution to the integral in eq. 11 comes from conditions at the critical size (the extension of the limits of integration from $-\infty$ to $+\infty$ is made because of this fact). The accuracy of this and other approximations used in nucleation theory is discussed in references 2 and 10. It should nevertheless be pointed that an analytical solution to eq. 11 can only be determined by using the Taylor's series form of W to perform the required integration.

W is a function of three variables - r_a, P''_a, and P''_b - so that the Taylor's series appropriate to a function of three independent variables must be used in the expansion. Expanding about conditions in the critical size nucleus, the three variable Taylor's series is

$$\begin{aligned} W = {} & W(r_{ac}, P''_{ac}, P''_{bc}) + (r-r_{ac})\partial W/\partial r_a\big|_c + (P''_a-P''_{ac})\partial W/\partial P''_b\big|_c \\ & + (P''_b-P''_{bc})\partial W/\partial P''_b\big|_c + (r-r_{ac})(P''_a-P''_{ac})\partial^2 W/\partial r_a \partial P''_a\big|_c \\ & + (P''_b-P''_{bc})(r-r_{ac})\partial^2 W/\partial P''_b \partial r_a\big|_c + (P''_b-P''_{bc})(P''_a-P''_{ac})\partial^2 W/\partial P''_b \partial P''_a\big|_c \\ & + \tfrac{1}{2}(r-r_{ac})^2 \partial^2 W/\partial r_a^2\big|_c + \tfrac{1}{2}(P''_a-P''_{ac})^2 \partial^2 W/\partial P''^2_a\big|_c \\ & + \tfrac{1}{2}(P''_b-P''_{bc})^2 \partial^2 W/\partial P''^2_b\big|_c + \text{higher order terms} \end{aligned} \qquad 54.$$

At the critical size the bubble radii are related to the pressure difference across the bubble surface as follows:

$$P''_{bc} + P''_{ac} - P_o = 2\sigma_a/r_{ac} = 2\sigma_b/r_{bc} \qquad 55$$

which is the condition of mechanical stability at the critical size (Laplace's equation). Using eqs. 55 and 53, the required partial derivatives in eq. 54 are the following:

$$\begin{aligned} W\big|_c &= 4/3\,\pi r_{ac}^2 F_a & \partial W/\partial P''_a\big|_c &= 0 \\ \partial^2 W/\partial r_a^2\big|_c &= -8\pi\sigma_a F_a & \partial^2 W/\partial r_a \partial P''_b\big|_c &= 0 \\ \partial W/\partial r_a\big|_c &= 0 & \partial^2 W/\partial P''^2_a\big|_c &= 4/3\,\pi r_{ac}^3 F_a/P''_{ac} \\ \partial^2 W/\partial P''_b \partial P''_a\big|_c &= 0 & \partial W/\partial P''_b\big|_c &= 0 \\ \partial^2 W/\partial P''^2_b\big|_c &= 4/3\pi r_{ac}^3 F_a/P''_{bc} & \partial^2 W/\partial r_a \partial P''_a\big|_c &= 0 \end{aligned} \qquad 56.$$

Substituting equations 56 into equation 54 and rearranging gives the Taylor's series equivalent of W in equation 53:

$$W = \pi r_{ac}^2 \sigma_a F_a 4/3 - 4\pi\sigma_a F_a (r_a - r_{ac})^2 + 2/3\pi F_a r_{ac}^3 ((P''_a - P''_{ac})^2/P''_{ac} + (P''_b - P''_{bc})^2/P''_{bc}) + \text{higher order terms} \qquad 57.$$

By substituting equations 50b and 48 in eq. 57, W can be expressed in terms of r_b by simply replacing σ_a by σ_b, F_a by F_b, and r_a by r_b.

The variable of integration in eq. 11 can be changed from x'' to r_a and r_b to give the following:

$$J = \frac{N}{(2\pi kT)^{\frac{1}{2}}} \left[\frac{P_a S_a(r_a)}{m_a^{\frac{1}{2}}} + \frac{P_b S_b(r_b)}{m_b^{\frac{1}{2}}} \right] \frac{1}{\frac{dx}{dr_a} \int_{-\infty}^{\infty} \frac{dr_a}{n(r_a)}} \qquad 58.$$

W must be expressed as a function of only r_a to evaluate the first term in brackets, and a function of only r_b to evaluate the second term in brackets.

The equation of state of the gas in the bubble is

$$x'' = (P''_a + P''_b) V''_b / kT.$$

Substituting equations 51 and 55 into the above equation gives the following:

$$x'' = 4/3\pi F_a (r_a^3 P_o + 2\sigma_a r_a^2)/kT \qquad 59.$$

Differentiating eq. 59 with respect to r_a and rearranging, one obtains

$$dx''/dr_a = 4\pi F_a r_a^2 (P''_a + P''_b) B/kT \qquad 60.$$

where B is defined as

$$B = 1-(1-P_o/(P''_a+P''_b))/3 \qquad 61.$$

Expressing the equation of state as a function of r_b, one obtains

$$x'' = 4/3\pi F_b \quad (r_b^3 P_o + 2\sigma_b r_b^2)/kT \qquad 62.$$

Differentiating eq. 62 with respect to r_b gives,

$$dx''/dr_b = 4\pi F_b r_b^2 (P''_a+P''_b)B/kT \qquad 63.$$

To perform the required integration in eq. 58, P''_a and P''_b must each be expressed as a function of r_a or r'_a so that W in eq. 57 will be a function of only one variable (r_a or r_b). There are, however, four variables and only two independent relations - equations 48 and 55. Unless an additional equation is available relating these four variables, eq. 58 cannot be evaluated analytically. It is now apparent why in a previous treatment of this problem (ref. 4) the assumption of only one volatile liquid was made, for this provides the additional condition needed to solve eq. 58.

When $P''_a >> P''_b$, eq. 55 can be written as

$$P''_a - P_o \approx P''_a + P''_b - P_o = 2\sigma_a/r_a = 2\sigma_b/r_b \qquad 64.$$

At atmospheric pressure P''_a will usually be much greater than P_o. However, if nucleation occurs at high pressure, P_o and P''_a may both be the same order of magnitude. For this reason P_o will be retained in eq. 64 with the understanding that it has a small effect at P_o=latm.

Near the critical size where P''_a and P''_{ac} are approximately the same order of magnitude (similarly for P''_b and P''_{bc}), the condition $P''_a >> P''_b$ implies that

$$P''^2_a/P''_{ac} >> P''^2_b/P''_{bc}.$$

The second term in brackets in eq. 57 can therefore be neglected compared to the first. With this simplifying assumption eq. 57 can be combined with equations 48, 50, and 64 to express W in terms of the single variable r_a or r_b.

Since,

$$2/3\pi F_a r^3_{ac}(P''_a-P''_{ac})^2/P''_{ac} = 4/3\pi F_a\sigma_a(r_a-r_{ac})^2(1-P_o/P''_{ac}) \quad 65,$$

eq. 57 can be expressed as a function of only r_a or r_b as follows:

$$W(r_a) = 4/3\pi r^2_{ac}\sigma_a F_a - (r_a-r_{ac})^2 4\pi\sigma_a F_a B_a \quad 66;$$

and

$$W(r_b) = 4/3\pi r^2_{bc}\sigma_b F_b - (r_b-r_{bc})^2 4\pi\sigma_b F_b B_a \quad 67.$$

In equations 66 and 67 $B_a \approx B$ because $P''_a >> P''_b$. The subscript "a" will therefore be dropped when re-writing equations 66 and 67 in the future.

After substituting equations 52a, 60, and 66 into eq. 58, one obtains

$$J_a = \frac{NP''_a A_a \exp(-4\pi F_a\sigma_a r^2_{ac}/3kT)}{(2\pi m_a kT)^{\frac{1}{2}} F_a B(P''_a+P''_b) \int_{-\infty}^{\infty} \exp(-4\pi\sigma_a F_a B(r_a-r_{ac})^2/kT)dr_a} \quad 68.$$

Cancelling terms in eq. 68 and evaluating the integral (a standard error function), it is seen that

$$J_a = NA_a\left(\frac{2\sigma_a}{\pi m_a F_a B}\right)^{-\frac{1}{2}} \frac{P''_a}{P''} \exp\left(-\frac{16\pi\sigma_a^3 F_a}{3kT(P''-P_o)^2}\right) \qquad 69$$

where $P''=P''_a+P''_b$. The second term in eq. 58 is similarly evaluated by substituting equations 52b, 63, and 67, evaluating the integral, and eliminating r_{bc} by using eq. 64. The result is

$$J_b = NA_b\left(\frac{2\sigma_b}{\pi m_b F_b B}\right)^{\frac{1}{2}} \frac{P''_b}{P''} \exp -\left(\frac{16\pi\sigma_b^3 F_b}{3kT(P''-P_o)^2}\right) \qquad 70.$$

Combining equations 69 and 70 and expressing $\sigma_b^3 F_b$ in terms of $\sigma_a^3 F_a$ by using eq. 50b, the nucleation rate at the interface between two immiscible liquids is,

$$J = N\left(\frac{2}{\pi\sigma_a^3 F_a B}\right)^{\frac{1}{2}} \left[\frac{P''_a A_a \sigma_a^2}{m_a^{\frac{1}{2}} P''} + \frac{P''_b A_b \sigma_b^2}{m_b^{\frac{1}{2}} P''}\right] \exp\left(-\frac{16\pi\sigma_a^3 F_a}{3kT(P''-P_o)^2}\right) \qquad 71$$

where $N = N_a^{2/3} + N_b^{2/3}$

The discussion on pages 8 to 10 emphasized that the smallest transfer area for an a molecule on a bubble formed entirely in liquid b may be taken as the surface area of a single a molecule. This suggests that the transfer areas (i.e., bubble surface areas) given by equation 52 can be alternatively expressed as follows:

$$S_a = 4\pi r_a^2 A_a + \Delta_a(1-A_a) \qquad 72a;$$

and

$$S_b = 4\pi r_b^2 A_b + \Delta_b(1-A_b) \qquad 72b.$$

Δ_a and Δ_b are the surface areas of the hard sphere a and b molecules. Expressing the bubble surface area by equation 72, though justified on physical grounds, really has no rigorous mathematical basis. Its only effect on the final result will be in the pre-exponential term in the integrated form of eq. 58. To show this equation 72 is substituted directly into eq. 58 and the integration performed. The resulting expression for the nucleation rate is the following:

$$J = N\left(\frac{1}{\pi^3 128\sigma_a^3 F_a B}\right)^{\frac{1}{2}}\left[\left(\frac{16\pi A_a\sigma_a^2 + (P''-P_o)^2(1-A_a)\Delta_a}{m_a^{\frac{2}{3}}}\right)\frac{P''_a}{P''}\right.$$
$$\left. + \left(\frac{16\pi A_b\sigma_b^2 + (P''-P_o)^2(1-A_b)\Delta_b}{m_b^{\frac{2}{3}}}\right)\frac{P''_b}{P''}\right]\exp\left(-\frac{16\pi\sigma_a^3 F_a}{3kT(P''-P_o)^2}\right) \qquad 73.$$

Equation 73 was obtained from eq. 58 by evaluating the pre-exponential term in the integrand at the critical size and then removing it from under the integral sign. This is permissible in view of the sharp maximum of the exponential term at the critical size. Eq. 73 reduces to eq. 71 when $\Delta_a = \Delta_b = 0$ in eq. 73.

Setting $\Delta_a = \Delta_b = 0$ will not in most cases effect the nucleation rate. Even if $\Delta_a(P''-P_o)^2(1-A_a)$ is the same order of magnitude as $16\pi\sigma_a^2 A_a$ in eq. 73, neither the nucleation rate nor temperature calculated from eq. 73 will be significantly different from that calculated using eq. 71. That is, there is a negligible difference in the numerical results obtained from equations 71 and 73.

It is interesting to compare the formula for the nucleation rate at a liquid-liquid interface derived in reference 4 (repeated as eq. 74 below) with equations 71 and 73.

$$J = N_a^{2/3} \left(\frac{2}{\pi o_a^3 F_a B}\right)^{\frac{1}{2}} \left[\frac{A_a \sigma_a^2}{m_a^{\frac{1}{2}}}\right] \exp\left(- \frac{16\pi\sigma_a^3 F_a}{3kT(P''-P_o)^2}\right) \qquad 74.$$

This equation was derived assuming that bubble growth was due solely to a molecules being absorbed on transfer area S_a for bubble formation as shown in figs. 3c and 6a. The important point to notice in eq. 74 is that if $M_a=1$, then $J=0$. But $M_a=1$ corresponds, as will be shown, to a spherical bubble formed in liquid b and tangent to the interface. The fact that $J=0$ then implies that no bubble will ever form in this way (at least by the mechanism of random molecular collisions). Yet this geometry should be permissible. This result would also occur in equations 71 and 73 by setting $A_b=0$ and $\Delta_b=0$ which is equivalent to assuming that no b molecules are in a nucleus formed at the interface (i.e., zero transfer area for b molecules).

A slightly inconsistent recommendation is made that the bubble gas pressure, P", is the sum of the partial pressures of a and b. The question, of course, is how can b molecules enter the nucleus if its transfer area is zero? This is best explained by noting that the nucleation rate given by eq. 74 was derived from an equation similar to eq. 1:

$$J_k = \frac{\beta}{\int_1^\infty \frac{dx}{S_a(x)n(x)}}$$

To produce eq. 74 from equations 66, 64, 52a and the above expression, β must be given by the following (if $P''=P''_a+P''_b$):

$$\beta = \frac{(P''_a+P''_b)}{(2\pi m_a kT)^{\frac{1}{2}}}$$

which does not seem quite right.

The problem is that there are <u>two</u> transfer areas instead of one and that eq. 1 should have been used to determine the nucleation rate. One can argue, however, that these "errors" have a small effect in that they appear only in the pre-exponential term in the expression for the nucleation rate. Nevertheless it will be shown that the absurd result $J=0$ can occur under certain limiting conditions in eq. 74.

The particular conditions which render equation 71 or equation 73 valid were determined in reference 4 (using eq. 74) in a rather elegant manner. Combing equations 46a, 47, and 55 together with the identity $\sin(\theta) = (1-\cos(\theta))^{\frac{1}{2}}$, the characteristic lens dimension, $\bar{a}$ in fig. 6a, can be expressed as follows:

$$\bar{a} = \frac{2\sigma_a}{(P''-P_o)}\left[1 - \frac{(\sigma_a^2+\sigma_{ab}^2-\sigma_b^2)^2}{4\sigma_a^2\sigma_{ab}^2}\right]^{\frac{1}{2}}$$

This formula was factored in reference 4 and appears as eq. 75 below:

$$\bar{a} = \frac{\sigma_{ab}}{(P''-P_o)}\left(\left[\left(\frac{\sigma_a+\sigma_b}{\sigma_{ab}}\right)^2 - 1\right]\left[1 - \left(\frac{\sigma_a-\sigma_b}{\sigma_{ab}}\right)^2\right]\right)^{\frac{1}{2}} \qquad 75.$$

From eq. 75 the conditions for determining the location of bubble formation at a liquid-liquid interface shown in fig. 3

are now seen to depend only on the appropriate surface and interfacial tensions. Depending on these values the following cases may mathematically occur:

1) $\bar{a}$ is real;

2) $\bar{a}$ is zero; and

3) $\bar{a}$ is imaginary.

Depending on whether the second term in brackets in eq. 74 is positive, zero, or negative gives the required conditions because physically $\sigma_{ab}<\sigma_a+\sigma_b$ always occurs.

$\bar{a}$ is real only when

$$\sigma_{ab} > |\sigma_a-\sigma_b| \qquad 76.$$

The lens radius is zero when

$$\sigma_{ab} = |\sigma_a-\sigma_b| \qquad 77$$

or alternatively when

$$\sigma_a = \sigma_b+\sigma_{ab} \qquad 78$$

or

$$\sigma_b = \sigma_a+\sigma_{ab} \qquad 79.$$

$\bar{a}$ is imaginary when

$$\sigma_a > \sigma_b+\sigma_{ab} \qquad 80$$

or

$$\sigma_b > \sigma_a+\sigma_{ab} \qquad 81.$$

These three conditions are discussed below.

1) <u>$\bar{a}$ is real</u>:

In this case equation 76 applies. A bubble exists between liquids <u>a</u> and <u>b</u> as illustrated in fig. 3c, and equation 71 or

equation 73 gives the expression for the nucleation rate.

2) $\bar{a}$ is zero:

Either of equations 78 or 79 apply in this case.

i. $\sigma_a' = \sigma_{ab} + \sigma_b$ 78

When equation 78 applies it can easily be shown that (see equations 46, 50, and 52)

$$F_a = \sigma_b^3/\sigma_a^3 \qquad 82a$$

$$F_b = 1 \qquad 82b$$

$$A_a = 0 \qquad 82c$$

$$A_b = 1 \qquad 82d$$

$$M_a = 1 \qquad 82e$$

$$M_b = -1 \qquad 82f.$$

Under these conditions equation 73 reduces to the following equation:

$$J = N\left[\left(\frac{\Delta_a(P''-P_o)^2}{m_a^{\frac{3}{2}}}\right)\frac{P''_a}{P''} + \left(\frac{16\pi\sigma_b^2}{m_b^{\frac{3}{2}}}\right)\frac{P''_b}{P''}\right]\frac{1}{(128\pi^3 B\sigma_b^3)^{\frac{1}{2}}}\exp\left(-\frac{16\pi\sigma_b^3}{3kT(P''-P_o)^2}\right) \qquad \text{eq. 83a.}$$

Equation 71 with $\Delta_a = 0$ becomes

$$J = N\left(\frac{2\sigma_b}{\pi m_b B}\right)^{\frac{1}{2}}\frac{P''_b}{P''}\exp -\left(\frac{16\pi\sigma_b^3}{3kT(P''-P_o)^2}\right) \qquad 83b.$$

Substituting equation 82 into eq. 74 gives, in addition, $J_k = 0$. Comparing equations 71 and 73 with 74 shows why this occurs. There is no transfer area for b molecules so that there is only one pre-exponential term in eq. 74 and this term is zero when

equation 78 is satisfied.

It may be recognized that equation 83b is the formula for homogeneous nucleation in liquid b for bubble growth as illustrated in fig. 3d (except N is now the number density of surface molecules). This is not surprising because $F_b=1$ and hence $V_b''= 4/3\pi r_b^3$ so that the nucleus is spherical of radius r_b.

The work to form the critical size nucleus is, from the exponential term in equation 82a (or 83b),

$$W = \frac{16\pi\sigma_b^3}{3(P''-P_o)^2} \qquad 84.$$

Equation 84 is exactly the formula which would be obtained for the work to form a spherical bubble of critical size in the bulk of liquid b. At the condition under present discussion, the bubble forms at the interface and is tangent to the surface because $\theta = 0$ and $\phi = 180$ when $M_a=1$ and $M_b=-1$.

ii. $\sigma_b = \sigma_{ab}+\sigma_a$ 79

When eq. 79 is satisfied, it can be shown that

$$F_a=1 \qquad 85a$$
$$F_b=\sigma_a^3/\sigma_b^3 \qquad 85b$$
$$A_a=1 \qquad 85c$$
$$A_b=0 \qquad 85d$$
$$M_a=-1 \qquad 85e$$
$$M_b=1 \qquad 85f.$$

Under the conditions given by equations 85, eq. 73 reduces to,

$$J= \frac{N}{(\pi^3 128 B\sigma_a^3)^{\frac{1}{2}}}\left[\left(\frac{16\pi\sigma_a^2}{m_a^{\frac{1}{2}}}\right)\frac{P_a''}{P''} + \left(\frac{\Delta_b(P''-P_o)^2}{m_b^{\frac{1}{2}}}\right)\frac{P_b''}{P''}\right]\exp\left(-\frac{16\pi\sigma_a^3}{3kT(P''-P_o)^2}\right) \qquad 86.$$

When $\Delta_b=0$, equation 71 reduces to

$$J = N\left(\frac{2\sigma_a}{\pi m_a B}\right)^{\frac{1}{2}} \frac{P''_a}{P''} \exp\left(-\frac{16\pi\sigma_a^3}{3kT(P''-P_o)^2}\right) \qquad 87.$$

The second term in brackets in eq. 86 is expected to be negligible compared with the first term because $P''_a >> P''_b$. Eq. 86 then further reduces to eq. 87.

The work to form the critical size bubble is

$$W = \frac{16\pi\sigma_a^3}{3(P''-P_o)^2} \qquad 88.$$

Equations 87 and 88 are exactly what one would obtain for homogeneous nucleation in the bulk of liquid a except that N would be the number density of a molecules and not the number density of molecules at the interface between the two liquids. In addition for homogeneous nucleation in the bulk of liquid a, only a molecules would be in the bubble so that $P''_a/P'' = 1$ and $P''_b/P'' = 0$.

A spherical bubble is formed when eq. 79 is satisfied because $F_a=1$ in eq. 50b. In addition $\phi=0$ and $\theta=180$ (from eqs. 46a and 46b) so that the bubble is tangent to the interface and surrounded by liquid a as illustrated in fig. 3b.

3) $\bar{a}$ is imaginary:

This is the most interesting situation because there is no rigorous mathematical limit to which eq. 71 or eq. 73 approaches. Moreover this condition is requently encountered in nature. Simply stated, when $\bar{a}$ is imaginary, a nucleus cannot form anywhere at the interface and must grow away from the inter-

face in the bulk of either liquids a or b (figs. 3a and 3e). Equations 80 and 81 are discussed separately below.

$$\text{i. } \underline{\sigma_a > \sigma_b + \sigma_{ab}} \qquad 80.$$

When equation 80 is satisfied, it can be shown that

$$M_a > 1,$$

$$M_b < -1,$$

and

$$F_b > 1.$$

But the cosine of an angle can never be greater than 1. Therefore there is no bubble configuration at the interface describable by the angles θ and ϕ, and hence no bubble exists at the interface (at least in a mathematical sense).

The fact that $F_b > 1$ implies that if a bubble could grow at the interface, the energy of its formation to the critical size would be less in the bulk of liquid b than at the interface. This is so because from equations 55 and 67 at $r=r_{bc}$

$$W = \frac{16\pi\sigma_b^3 F_b}{3(P''-P_o)^2} \qquad 89.$$

while the work to form a bubble of critical size in the bulk of liquid b is given by eq. 84 which is smaller than eq. 89 by F_b. In addition the nucleation rate is greater by a factor of 10^6 when a nucleus forms homogeneously within the bulk of a liquid. Both of these factors tend to increase the probability that nucleation will occur in the bulk of liquid b rather that at the interface. The choice is essentially between the locations illustrated in figs. 3c, 3d, and 3e.

For homogeneous nucleation in the bulk of liquid b there are

no a molecules in the bubble so that $P_a''=0$ and $\Delta_a=0$. The bubble is spherical which implies that $A_b=1$. Equation 73 then becomes

$$J = N_b\left(\frac{2\sigma_b}{\pi m_b B}\right)^{\frac{1}{2}} \exp\left(-\frac{16\pi\sigma_b^3}{3kT(P_b''-P_o)^2}\right) \qquad 90.$$

Equation 80 is most likely to be satisfied by water-fuel emulsions stabilized by an emulsifying agent. For such emulsions $P_a'' >> P_b''$ (liquid a is water and b is fuel). Therefore, the arguments presented on pages 8 to 10 apply in this case as measured superheat temperatures are just too low to be explained by homogeneous nucleation in liquid b. This means there must be a non-zero transfer area for a molecules. Assuming that the bubble forms close enough to the interface so that the dominant growth mechanism is that of random molecular absorption on the bubble surface (i.e., diffusion is neglected), the nucleation rate may be approximated by equation 83a. The suggestions are then the following: When $P_a'' >> P_b''$, equation 83a or equation 83b($\Delta_a=0$ in eq. 83a) will apply. If, however, $P_a'' << P_b''$, the expected result is equation 90 ($P_a''=0$ and $A_b=1$ in eq. 73). Experimental results are in quite good agreement with eq. 83a($P_a'' >> P_b''$) lending support to these recommendations.

ii. $\sigma_b > \sigma_a+\sigma_{ab}$ 81

When this condition is satisfied, it can be shown that

$$M_a<-1$$

$$M_b>1$$

$$F_a>1.$$

When $F_a>1$ it takes less work to form a spherical bubble of critical

size in the bulk of liquid a than at the interface. This is so because for a bubble dividing the interface (fig. 3c)

$$W = \frac{16\pi\sigma_a^3 F_a}{3(P''-P_o)^2} \qquad 91.$$

which is larger than eq. 88 by F_a. The use of eq. 88 suggests that $F_a=1$ (spherical bubble), $A_a=1$, and $P''_b=0$ (no b molecules in the nucleus) for a bubble forming away from the interface in the bulk of liquid a. Substituting these conditions into eq. 73, it is seen that

$$J = N_a\left(\frac{2\sigma_a}{\pi m_{a_B}}\right)^{\frac{1}{2}} \exp\left(-\frac{16\pi\sigma_a^3}{3kT(P''_a-P_o)^2}\right) \qquad 92.$$

If $P''_a \ll P''_b$, the same dilemma will arise as discussed before: the bubble must grow close enough to the interface for b molecules to enter. This means that the nucleus must be in contact with the interface. The above arguments can be used to show that equation 86 will approximate the nucleation rate in this case. This suggests that when $P''_b \gg P''_a$ and $\sigma_b \geq \sigma_a+\sigma_{ab}$, equation 86 can be used to approximate the nucleation rate.

4. Summary of Theoretical Discussion

Nucleation at the interface between two immiscible liquids of which the dominant growth mechanism is random molecular absorption on the bubble surface has been described. The theoretical developments are summarized below.

1) $\sigma_{ab} > \sigma_a - \sigma_b$ 76

$$J = N\left(\frac{1}{\pi^3 128\sigma_a^3 F_a B}\right)^{\frac{1}{2}}\left[\left(\frac{16\pi A_a\sigma_a^2 + (P''-P_o)^2(1-A_a)\Delta_a}{m_a^{\frac{1}{2}}}\right)\frac{P''_a}{P''} + \left(\frac{16\pi A_b\sigma_b^2 + (P''-P_o)^2(1-A_b)\Delta_b}{m_a^{\frac{1}{2}}}\right)\frac{P''_b}{P''}\right]\exp\left(-\frac{16\pi\sigma_a^3 F_a}{3kT(P''-P_o)^2}\right) \quad 73.$$

When $\Delta_a=0$ and $\Delta_b=0$,

$$J = N\left(\frac{2}{\pi\,\sigma_a^3 F_a B}\right)^{\frac{1}{2}}\left[\left(\frac{A_a\sigma_a^2}{m_a^{\frac{1}{2}}}\right)\frac{P''_a}{P''} + \left(\frac{A_b\sigma_b^2}{m_b^{\frac{1}{2}}}\right)\frac{P''_b}{P''}\right]\exp\left(-\frac{16\pi\sigma_a^3 F_a}{3kT(P''-P_o)^2}\right) \quad 71.$$

$$F_a=(\sigma_a^3(2-3M_a+M_a^3)+\sigma_b^3(2-3M_b+M_b^3))/(4\sigma_a^3) \quad 50a$$

$$M_b=(\sigma_b^2+\sigma_{ab}^2-\sigma_a^2)/(2\sigma_b\sigma_{ab}) \quad 46b$$

$$M_a=(\sigma_a^2+\sigma_{ab}^2-\sigma_b^2)/(2\sigma_a\sigma_{ab}) \quad 46a$$

$$B=1-(1-P_o/P'')(1/3) \quad 61$$

$$A_a=(1-M_a)^{\frac{1}{2}} \quad 52b$$

$$A_b=(1-M_b)^{\frac{1}{2}} \quad 52a$$

$$N=N_a^{2/3}+N_b^{2/3} \quad 7$$

$$P''=P''_a+P''_b$$

A lens shpaed bubble will form at the interface between the two liquids (fig. 3c).

2) $\sigma_a = \sigma_b+\sigma_{ab}$ 78

$$A_a=0$$

$$A_b=1$$

$$J = N\left[\left(\frac{(P''-P_o)^2\Delta_a}{m_a^{\frac{3}{2}}}\right)\frac{P''_a}{P''} + \left(\frac{16\pi\sigma_b^2}{m_b^{\frac{3}{2}}}\right)\frac{P''_b}{P''}\right]\left(\frac{1}{\pi^3 128 B\sigma_b^3}\right)^{\frac{1}{2}} \exp -\left(\frac{16\pi\sigma_b^3}{3kT(P''-P_o)^2}\right) \qquad 83a.$$

When $\Delta_a=0$, equation 83b results. There is a negliglble difference between eq. 83a and 83b. (See fig. 3d).

3) $\sigma_a > \sigma_b+\sigma_{ab}$ 80

$F_b>1$

$M_a>1$

$M_b<-1$

3a) $P''_a<<P''_b$

$$J = N_b\left(\frac{2\sigma_b}{\pi m_b B}\right)^{\frac{1}{2}} \exp\left(-\frac{16\pi\sigma_b^3}{3kT(P''_b-P_o)^2}\right) \qquad 90$$

(See fig. 3e).

3b) $P''_a>>P''_b$

Equation 83a (or 83b) above applies. Equation 80 is replaced by the following: $\sigma_a \geq \sigma_b+\sigma_{ab}$.

4) $\sigma_b = \sigma_a+\sigma_{ab}$ 79

$F_a=1$

$A_a=1$

$A_b=0$

$M_a=-1$

$M_b=1$

$$J = N\left(\frac{1}{\pi^3 128 B\sigma_a^3}\right)^{\frac{1}{2}}\left[\left(\frac{16\pi\sigma_a^2}{m_a^{\frac{1}{2}}}\right)\frac{P''_a}{P''} + \left(\frac{(P''-P_o)^2\Delta_b}{m_b^{\frac{1}{2}}}\right)\frac{P''_b}{P''}\right]\exp\left(-\frac{16\pi\sigma_a^3}{3kT(P''-P_o)^2}\right) \qquad 86.$$

When $\Delta_b=0$ in eq. 86, <u>equation 87</u> results. There is a negligible difference between these two equations. (See fig. 3b).

5) $\sigma_b > \sigma_a+\sigma_{ab}$ 81

$F_a>1$

$M_a<-1$

$M_b>1$

5a) $P''_a >> P''_b$

$$J = N\left(\frac{2\sigma_a}{\pi m_a B}\right)^{\frac{1}{2}} \exp\left(-\frac{16\pi\sigma_a^3}{3kT(P''_a-P_o)^2}\right) \qquad 92$$

5b) $P''_a << P''_b$

<u>Equation 86</u> (or 87) applies. Eq. 81 can be replaced by the following condition: $\sigma_b \geq \sigma_a+\sigma_{ab}$.

III. Experimental Program

1. Basic Considerations

The purpose of the experimental program was to determine which of equations 76 to 81 was satisfied for the particular water-fuel emulsions used here, and whether the corresponding expression for the nucleation rate could be used to predict the temperature at which nucleation would occur during burning of the emulsified fuel droplet.

The method used here consisted of preparing an emulsion of two liquids, a and b, and then heating a sample drop. Such a drop is shown schematically in fig. 7a. The interface of the internal phase and surrounding liquid can be viewed as a flat interface (illustrated in fig. 7b). It is assumed that the tiny droplets of liquid a are far enough apart so that the surrounding liquid can be considered as an infinite mass. The geometry of fig. 7b then becomes that of fig. 3.

For an emulsion drop heated in air, the maximum temperature will be limited by the boiling point of liquid b. Unless the nucleation temperature at the interface between the two liquids is lower than this temperature, nucleation will not occur. The b liquid may also have to be superheated. This suggests the classic nucleation experiment in which a drop of a test liquid is injected in the bottom of a column filled with a heavier immiscible liquid under a temperature gradient. The rising drop is progressively heated until it explodes. The maximum droplet temperature attainable in this experiment is the limit of super-

heat of liquid b (assuming the boiling point of the column fluid is higher than this temperature). Since the limit of superheat of a liquid is usually around 90% of its critical temperature, considerable superheat of the liquid can therefore be sustained in the emulsion. One is not limited by the boiling point of liquid b in this experiment.

The design of the apparatus is basically that described in reference 11.

2. Experimental Apparatus and Method

A schematic illustration of the apparatus is shown in fig. 8. The column consisted of a pyrex tube 4.2cm inside diameter and 68cm long. The central 37cm was wound with 32 turns of nichrome wire and cemented in place with Sauereisen cement. The spacing between turns varied from 2cm at the lower end to .5cm at the upper end. Power to the nichrome wire was provided by an AC voltage supply controlled by a variac. Temperature was measured by one #28 gage copper-constantan thermocouple enclosed in a "L" shaped pyrex tubing jacket inserted directly into the column heating liquid. The thermocouple was connected to a Leeds & Northrup Model 8696 potentiometer and calibrated to about .1C.

A #10 rubber stopper was inserted into each end of the column. The thermocouple tubing jacket and a condenser were fitted into the top robber stopper. The condenser reduced the amount of column heating liquid lost by vapor generation during heating and prevented harmful vapors from entering the laboratory. A nitrogen gas atmosphere above the heating liquid was provided

to reduce oxidation and subsequent darkening of the column heating liquid (glycerine in this case). Efforts were made to insure that atmospheric conditions were maintained by only lightly purging the gas above the heating liquid.

Droplet injection was by a hypodermic needle. A 1/8 inch diameter by 1.5 inch long brass tube with a 3/4 inch diameter by 3/4 inch long brass cylinder soldered on the end was fitted into the center of the bottom rubber stopper. A rubber septum was placed over the brass cylinder which could be punctured by the needle (see fig. 8). A number 22 gage hypodermic needle 2 inches long fitted with a 1cc glass syring was used to inject the drops.

Because of the necessity of knowing accurately fuel properties, only pure fuels were used in the emulsions. Test droplets consisted of water-in-fuel emulsions. The emulsions were prepared by pouring a selected volume percentage of water in the fuel and mixing by a counter rotating propeller (fig. 9). Because of the high water-fuel interfacial tension (typically between 30 dynes/cm and 60 dynes/cm at 20C), it was necessary to stabilize the emulsion by adding an emulsifying agent. Otherwise the water would coalesce and collect in the bottom of the mixing beaker. The emulsifying agent was first mixed in the fuel and the water added later. Various samples containing between 1% and 2% emulsifying agent were prepared. The emulsifying agent was a mixture of 60% Span 85 and 40% Tween 85 (available from ICI America, Inc.). This particular mixture was experimentally found to stabilize higher alkane-water emulsions for at least

15 minutes at room temperature which was ample time to draw out a freshly made sample and inject a drop into the heating column. For other water-fuel combinations this particular emulsifying agent proved unsatisfactory. In particular a methanol-water emulsion could not be prepared in this way without the water coalescing.

The emulsions were made up of 83% fuel, 15% water and 2% emulsifying agent (by volume). The four water-fuel emulsions tested were the following:

1) water-decane;
2) water-dodecane;
3) water-tetradecane; and
4) water-hexadecane.

A test run proceeded by stabilizing a temperature gradient in the column and injecting a drop of the test emulsion. Meaurements consisted of recording the height of explosive boiling and the corresponding temperature. Explosions of large drops (> 2mm diameter) occasionally upset the column temperature gradient, and about 15 minutes to 30 minutes was required to re-stabilize the gradient. Fig. 10 shows a typical temperature gradient in the column (the temperature was adjusted to 286C at the top for a pure decane experiment). The temperature gradient was very flat at the top of the column, varying about 2C per 10cm. Whenever possible, the gradient was adjusted to cause explosions in this region.

No liquid is currently available which is immiscible both with

water and the fuels listed on the previous page, heavier than both, and with a boiling point greater than about 300C. The best liquid for use as a heating medium appeared to be glycerine which, unfortunately, is very soluble in water. A certain amount of surface dissolution of the water into the glycerine therefore had to be allowed to obtain nucleation temperatures by the method used here. Nevertheless, if it is assumed that nucleation occurs at a water-fuel interface within the drop, the corresponding temperature should be predictable from the theory presented here. The assumption is being made that a pure fuel shell surrounds the internal emulsion and no water can penetrate the fuel glycerine interface.

Additional experiments were run using pure hydrocarbon drops to test existing theories and to become familiar with the operation of the apparatus. The hydrocarbons were obtained from Humphrey Chemical Co. and of 99.6% purity or better. The following pure liquids were used: n-pentane; n-hexane; benzene; n-octane; and n-decane.

3. Experimental Results

Tables I and II list the experimentally measured superheat temperatures for the pure hydrocarbons and emulsions tested.

The nucleation temperatures of the pure hydrocarbons are completely consistent with values reported in the literature. In all cases the injected droplets exploded with a sharp report, the largest droplets (~2mm diameter) actually shaking the apparatus.

Droplet explosions for the pure hydrocarbons occured in a

very narrow temperature range. Stating an actual mumerical bound is somewhat fortuitous. As an example, for the pure n-pentane drops the thermocouple was positioned at the observed level of explosion. For all injected n-pentane drops, this level did not have to be changed because all drops exploded at the same height.

The temperatures listed in Table I represent an average of the recorded values and are accurate to within at least $\pm$ 1C.

The superheat temperature of n-decane was somewhat difficult to obtain. The measured value of about 283C is only 7C lower than the boiling point of glycerine. At this high temperature, stress cracks in the glass column were observed, and on one occasion the bottom of the pyrex tube literally broke off. The glycerine could not be maintained for more than $\frac{1}{2}$ hour at 283C before such trouble began to occur. However, once the proper gradient was established, and working swiftly, the superheat temperature of n-decane exhibited the same narrow range of explosive vaporization as the other hydrocarbons tested. Higher alkanes such as dodecane, hexadecane, and tetradecane have theoretical limits of superheat well in excess of 300C which just cannot be measured using glycerine as the heating medium. One would also be better off using a quartz column to support such temperatures. The highest superheat temperature ever measured at latm was 287C for cyclo-octane (reference 11). Needless to say the apparatus must have pushed to its limit to measure this temperature.

Injected droplet size was determined by measuring the rate

rise of a selected drop over a specified distance at a given temperature. The low Reynolds number solution of the terminal velocity of a liquid drop rising freely in an immiscible heavier liquid as derived in reference 12 was then used to correlate the measured rate of rise with the drop diameter. Droplet diameters for both the pure fuels and emulsions ranged between .5mm (500 microns) and about 2mm (2000 microns). For droplets larger than about 2mm diameter thermal equilibrium cannot be assumed (ref. 13). Data from drops of this size are not included in Tables I and II.

Internal dispersed phase (water) size of the emulsions was difficult to determine. Examination of a typical emulsion sample under a microscope at room temperature revealed some coalescence and internal motion. Generally, though, the order of magnitude of the internal water drop diameters appeared to range from about .01mm to .1mm. For even the smallest drops the assumption of a flat plane interface for nucleation is a good one because the diameter of a spherical nucle of critical size is about 10^{-7}cm, and $10^{-3} >> 10^{-7}$. Techniques for varying the internal phase size of emulsions, as well as photomicrographs of typical water-fuel emulsions, are given in reference 14.

Rising emulsion drops left a visible trail behind them. This indicated that water was slowly dissolving in the glycerine. Some settling of the water was also observed. As a droplet rose, the formation of a visible interface between the clear fuel and the milky internal emulsion was seen. An illustration of this is

shown in fig. 11. Whether this interface was formed as a result of drainage or settling of the heavier water, or a combination of both, is not known. In any case this was more pronounced in the smaller droplets (i.e., less than around .5mm diameter). For this size drop,water dissolution was so pronounced that before the droplet even reached its nucleation temperature it had become completely clear indicating that all the water had dissolved at the surface. The resulting pure fuel drop would then rise right to the top of the column without exploding. It was, therefore, necessary to have the injected droplet large enough so that there would still be some of the internal emulsion left by the time the droplet reached its nucleation temperature. In this regard, the size of the injected droplet rather than the percentage of water in the emulsion is more important.

Emulsions with 7% water and 1% emulsifying agent were also tested. No change in the maximum observed nucleation temperature was detected. There also appeared to be no dependence of the nucleation temperature on injected droplet diameter. The wide variety of internal water sizes described above also provide evidence of the independence of the nucleation temperature on droplet size. These observations are consistent with the theory presented before and the data reported in the literature.

Emulsion explosions were much less violent than pure fuel explosions. Rather than a sharp report, an almost inaudible "puff" accompanied each explosion.

Fully 90% of the injected emulsion droplets were observed to have air bubbles attached to them. This was due to the counter

rotating propeller causing significant cavitation in the fuel in the mixing beaker. Expansion of the air bubbles on the rising drops could be visually followed. These expansions occured within the first 5cm of the heated section of the column and were thus easy to detect. The column temperature gradient was temporarily upset by this and usually required 15 minutes to re-stabilize.

Even without attached air bubbles, droplet explosions of the fuel emulsions appeared to occur over a much wider temperature range than the pure liquids. Imperfectly wetted foreign particles in particular can lower superheat temperatures. Table II lists the highest recorded temperature for the particular water-fuel emulsion tested (in recording only the highest measured temperature, the reader is reminded of the work described in references 13 and 15).

IV. Discussion of Results

1. Surface Tension

By determining conditions which would result in real and imaginary solutions to the equation for the "radius" of a vapor lens at a liquid-liquid interface - eq. 75 - criteria were formulated for determining where a nucleus of critical size would appear. These criteria were found to depend only on the surface and interfacial tensions of the mutually saturated liquids.

Surface tension data of mutually saturated liquids generally do not exist. Most data reported in the literature are for liquids saturated either with their own vapor , or in air. The assumption will be made that the error in using the pure liquid component

surface tensions, σ_a and σ_b, is small.

The surface and interfacial tension variation with temperature must be known to use any of the formulas for the nucleation rate previously derived. Because these data are usually not available at liquid superheat temperatures, it is necessary to extrapolate to these temperatures. The error incurred by this extrapolation accounts for the dominant error in the prediction of nucleation temperatures.

Pure liquid surface tension values covering a wide variety of liquids appear in reference 16. Data for all liquids reported are given in the range of about 20C to 150C. For extrapolation to higher temperatures, it is useful to correlate these data with the following formula:

$$\sigma = \sigma_o(1-T/T_c)^n \qquad 93$$

where T_c is the critical temperature and σ_o and n are constants whose numerical values depend on the particular liquid. Correlations in the form of eq. 93 for all liquids studied here, except benzene and water, were found in the literature. For benzene and water a computer library subroutine was used to correlate the data given in reference 17 (for water) to a least squares curve. Values of the critical temperature were taken from reference 18. Appendix I lists the constants in eq. 93 and the least squares constants of the equation

$$\sigma = a_o + a_1 T + a_2 T^2 + \cdots \qquad 94$$

for benzene and water.

Interfacial tension data at high temperature were virtually non existant except for decane-water. The interfacial tension at only 20C could be located for tetradecane. For hexadecane-water and dodecane-water no values at any temperature could be found. The extent of the interfacial tension data for the emulsions tested is summarized in Table III below.

Table III
Interfacial Tension

Water-Tetradecane: σ_{ab} = 52.2 dynes/cm (@20C) (ref. 19)

Water-Decane: $\sigma_{ab} = 50.066 + .0027247P_o - .1205(T-298.15)$ (ref.20)

A formula relating the interfacial tension to the pure liquid component surface tensions was derived in ref. 21:

$$\sigma_{ab} = \sigma_a + \sigma_b - 2(\sigma_a^d \sigma_b^d)^{\frac{1}{2}} \qquad 95.$$

The last term in eq. 95 represents the dispersion force component of the interfacial tension. For the hydrocarbons used here this is equal to the pure liquid surface tension (ref. 21) so that $\sigma_b^d = \sigma_b$. The dispersion component of water, σ_a^d, was estimated in reference 9 to be

$$\sigma_a^d = K(\rho_l - \rho_v)^4$$

where K is a constant and ρ_l and ρ_v are liquid and vapor densities of water respectively. Combining this with eq. 95 gives the relation between surface and interfacial tension at a water-fuel interface and its subsequent variation with temperature:

$$\sigma_{ab} = \sigma_a + \sigma_b - 2(\sigma_b K(\rho_2 - \rho_v)^4)^{\frac{1}{2}} \qquad 96.$$

K is determined from a known value of σ_{ab} at one temperature:

$$K = \left[\frac{\sigma_{ao}+\sigma_{bo}-\sigma_{abo}}{2}\right]^2 \frac{1}{\sigma_{bo}(\rho_2 - \rho_v)^4} \qquad 97$$

where the subscript "o" denotes the reference temperature at which σ_{ab} is known.

For a tetradecane-water interface at 25C, σ_a=71.965dyne/cm, σ_b=26.126dyne/cm, and σ_{ab}=52.2dyne/cm. From eq. 97 (and thermodynamic tables for water properties), it is found that $K = 20.401\ cm^{12}/g^3\text{-}sec^2$. Similarly for a water-decane interface it can be shown that $K = 21.79\ cm^{12}/g^3\text{-}sec^2$, and for octane-water, $K = 22.8\ cm^{12}/g^3\text{-}sec^2$. These results suggest that the interfacial tensions of alkane-water systems do not differ greatly.

The location of bubble formation can now be determined from the conditions summarized on pages 43 to 45. Consider as an example a water-tetradecane emulsion. The highest measured nucleation temperature is about 260C (Table II). At this temperature $\sigma_a \approx 23.85$ dyne/cm, $\sigma_b \approx 7.9699$dyne/cm, and from eq. 96 with $K=20.401 cm^{12}/g^3\text{-}sec^2$, $\sigma_{ab} \approx 17.078$dyne/cm. Since

$$17.078 > |23.85-7.9699| = 15.88,$$

eq. 76 is satisfied. This means that one should expect a bubble to form between a water-tetradecane interface as illustrated in fig. 3c. Equation 73 or eq. 71 then provides the expression

for the nucleation rate. Similarly for a decane-water interface at 230C, $\sigma_a \approx 30.97$dyne/cm, $\sigma_b \approx 5.787$dyne/cm, and from Table III $\sigma_{ab} \approx 25.366$dyne/cm. Since

$$25.366 > |30.97 - 5.787| = 25.183,$$

eq. 76 is again satisfied (though just barely).

It is interesting to note that equations 76 to 81 are also the conditions for determining whether one liquid will spread on another. A detailed discussion of this will not be given here (see ref. 22). Briefly when eq. 76 is satisfied, a drop of liquid b on liquid a will form a lens. Equations 80 and 81, of which equations 78 and 79 are limiting cases, are the conditions of spreading of one liquid on another. For example, when eq. 80 is satisfied, a drop of liquid b on liquid a will immediately spread on the surface of a. This is equivalent to a drop of b resting on the surface of a with a zero contact angle. A similar explanation applies to eq. 81 for a drop of liquid a on liquid b. The implication is that when a surface is completely wetted by another liquid so that equations 80 or 81 applies, a spherical bubble will form either in the bulk of the wetting liquid (fig.3e) or at the interface surrounded by the wetting liquid (fig. 3d), depending on which liquid is more volatile.

For a water-decane interface at 20C, the data in Table III and Appendix I indicate that eq. 76 is satisfied. From the above discussion this means that a drop of decane will rest as a lens on the water, which is easily verified. This can also be verified for the other water-fuel systems in Table II.

When 2% by volume of emulsifying agent is mixed with any of the pure hydrocarbons listed in Table II, and a drop of this hydrocarbon-emulsifying agent mixture placed on water, the drop spreads instantly on the water surface. Eq. 76 is no longer satisfied and the spreading condition, eq. 80, describes the water-fuel interface. The stabilizing effect surfactants have on emulsions is due primarily to a lowering of the interfacial tension (the emulsifying agent being absorbed on the water-fuel interface). Although no measurements were made here of the interfacial tension at a water-fuel interface, it is apparent that if such data were taken, very low interfacial tensions would be measured.

Depending on the surfactant, it is possible to lower the interfacial tension from a typical value of 50dyne/cm to less than 1dyne/cm at 20C. Such a dramatic decrease of interfacial tension will change the location of bubble growth from a lens forming between the water-fuel interface (fig. 3c) to spherical bubble formation at the interface or in the bulk of the fuel. When this occurs, it is not necessary to actually know a numerical value of the interfacial tension. This is so because the work to form a spherical bubble depends only on the pure component surface tension of the liquid in which the bubble grows (i.e., equations 84, 88, and 89).

To determine the nucleation rate of an emulsion stabilized by a surfactant, it is only necessary to know which liquid spreads on the other, a condition which is sure to be satisfied. The

relatively high surface tension of water compared to the pure fuels examined here, and the fact that P''_a(water) >> P''_b(fuel), indicate that eq. 80 is satisfied. At temperatures greater than 200C, σ_a > 20dyne/cm, σ_b < 10dyne/cm, and σ_{ab} is conservatively less than 2dyne/cm when an emulsifying agent is added to the fuel. These estimates show that the fuel will still spread on water at this temperature.

Therefore, for the water-fuel emulsions listed in Table II (and probably for most pure hydrocarbon-water emulsions stabilized by an emulsifying agent),

$$\sigma_a > \sigma_b + \sigma_{ab} \qquad 80$$

and

$$J = N \frac{1}{(\pi^3 128 B \sigma_b^3)^{\frac{1}{2}}} \left[\left(\frac{\Delta_a (P''-P_o)^2}{m_a^{\frac{2}{3}}} \right) \frac{P''_a}{P''} + \left(\frac{16\pi\sigma_b^2}{m_b^{\frac{2}{3}}} \right) \frac{P''_b}{P''} \right] \exp\left(- \frac{16\pi\sigma_b^3}{3kT(P''-P_o)^2} \right) \qquad 83a$$

$$P'' = P''_a + P''_b$$

$$N = N_a^{2/3} + N_b^{2/3} \qquad 7.$$

For pure hydrocarbons rising in glycerine, $\sigma_g > \sigma_b + \sigma_{gb}$ and $P''_b >> P''_g$ so that the nucleation rate is given by eq. 90:

$$J = N_b \left(\frac{2\sigma_b}{\pi m_b B} \right)^{\frac{1}{2}} \exp\left(- \frac{16\pi\sigma_b^3}{3kT(P''_b-P_o)^2} \right) \qquad 90.$$

The above discussion indicates that there are two possible advantages in using an emulsifying agent in the preparation of water-fuel emulsions: 1) the emulsion will be stabilized at least for the time of the experiment; and 2) the resulting decrease in

the interfacial tension causes a change in the nucleation mechanism to the extent that the corresponding equation for the nucleation rate is independent of the interfacial tension.

Surfactant absorption at a water-fuel interface might suggest that the pure liquid component surface tension does not change appreciably. This hypothesis was tested by measuring the limit of superheat of n-pentane and n-decane each mixed with 2% emulsifying agent (60% Span 85 and 40% Tween 85). Superheat temperatures were nearly the same as for the pure liquids, ranging between 145C-147C for n-pentane and 280C-285C for n-decane. Given a nucleation rate and temperature, eq. 90 can be solved for surface tension. Because the measured superheat temperatures were nearly the same as that of the pure fuels, the pure fuel surface tension is essentially unaffected by the addition of the surfactant used in this study.

The choice of a heating medium depends on whether eq. 81 is satisfied. The hydrocarbons used here spread on glycerine indicating that eq. 81 is indeed satisfied. In addition since $P''_b >> P''_g$, nucleation will occur within the bulk of the injected fuel drop (homogeneous nucleation), and not at the fuel glycerine interface. The results in Table I verify this. A rising emulsion drop can therefore be modelled as a droplet burning in air except that now the droplet temperature is able to reach its limit of superheat and not just its boiling point. The advantages of this are obvious particularly in light of the results shown in Table II.

2. Vapor Pressure

The component gas partial pressure in a nucleus of critical size is not its equilibrium vapor pressure, but is slightly less. This is due both to bubble curvature and the fact that the external liquid pressure is at the ambient rather than the component equilibrium vapor pressure.

A nucleus of critical size is in chemical equilibrium. Accordingly for the ith component,

$$u_i' = u_i''$$

or

$$du_i' = du_i'' \qquad 98.$$

Eliminating the chemical potential between eq. 98 and eq. 19 results in the following:

$$\frac{V_i'}{x_i'} dP_i' = \frac{V_i''}{x_i''} dP_i'' \qquad 99.$$

Since $V_i'/x_i' = MW_i/(\rho_\ell' N_o)$ and $V_i''/x_i'' = MW_i/(\rho_\ell'' N_o)$ where MW_i is molecular weight, N_o is Avogadro's number, and ρ_ℓ is density, eq. 99 can be re-written as

$$dP_i''/\rho_\ell'' = dP_i'/\rho_\ell'$$

Assuming an incompressible liquid (ρ_ℓ' is constant) and an ideal gas so that $P_i'' = \rho_\ell'' RT$, the above equation can be integrated from the reference equilibrium vapor pressure at which $P_i' = P_{ie}''$ to conditions at the critical size where $P_i' = P_o$ and $P_i'' = P_{ic}''$. The result of this integration is the following:

$$P''_{ic} = P''_{ie} \exp(-\rho''_{\ell}(P''_{ie}-P_o)/(\rho'_i P''_{ie})) \qquad 100.$$

As in reference 5, the exponential term is expanded in a Taylor's series and the first three terms retained. Eq. 100 can then be put in the following form:

$$P''_{ic} = (P''_{ie}-P_o)\alpha_i + P_o \qquad 101a$$

where

$$\alpha_i = (1- \frac{\rho''_i}{\rho'_i} + \tfrac{1}{2}(\frac{\rho''_i}{\rho'_i})^2) \qquad 101b.$$

Eq. 101 provides a good approximation to the gas pressure of the ith component in the critical sized bubble. For the liquids used here $\alpha_i > .9$ at their limits of superheat (e.g., for water at 305C, $\alpha_i \approx .979$). Therefore, the component gas partial pressures in the bubble are nearly the same as their equilibrium vapor pressures.

The equations given in Appendix II relate the equilibrium vapor pressure of the liquids used here to temperature. These equations were obtained by curve fitting data available in various handbooks of thermodynamic properties.

When data were available, liquid and vapor densities of the hydrocarbons were fit to a least squares formula. When not available, α_i was set equal to .915 as recommended in reference 11. In either case the correction given by eq. 101 has a small effect on predicting nucleation temperatures using equations 83a and 90.

3. Nucleation Rate and Description of Solution Method

Equations 83a and 90 can be used to determine the nucleation

rate at a given temperature. This is a straightforward calculation because J is an explicit function of temperature. However, to calculate a temperature, equations 83a and 90 must be solved by trial and error. In addition it is necessary to know what nucleation rate corresponds to given experimental conditions. This can be adequately estimated if it is assumed that a droplet will boil if just one nucleus of critical size is formed in that droplet.

The usual procedure (refs. 5 and 11) is to assume that a collection of N drops is heated at a constant rate dT/dt (deg/sec). This can be controlled experimentally. (Even if dT/dt is some function of time, little error will result by using a suitable average value). Since J is the number of nuclei of critical size formed per unit volume and time, and V is the volume per drop, the following rate equation can be written:

$$JNV + dN/dt = 0 \qquad 102.$$

The first term represents the number of exploding drops per unit time, and the second term represents the change in the number of drops due to these explosions. Because $dN/dt = (dT/dt)dN/dT$, eq. 102 becomes

$$JdT = (-(dT/dt)/V)dN/N \qquad 103.$$

The numerical solution of equations 83a and 90 to be presented shortly indicate that over a wide range of nucleation rates, the temperature variation of J is approximately exponential (i.e., a plot of lnJ vs. T is a straight line). It is therefore

a good approximation to take

$$J \approx J_o \exp((d\ln J/dT)T) \qquad 104.$$

where $d\ln J/dT$ is a constant. Substituting equation 104 into 103 and integrating between $N=N_o$ and $T=T_o$ (initial number of drops at $T=T_o$) to $N=N_s$ and $T=T_s$ (the number of drops which have not yet exploded at temperature T_s) gives,

$$J(T_s)-J(T_o) = -(((d\ln J/dT)dT/dt)/V)\ln(N_s/N_o).$$

J is a very strong function of temperature so that T_o need be only a few degrees lower than T_s for $J(T_s) >> J(T_o)$. Incorporating this approximation in the above equation gives, [illegible] drops have exploded [illegible] and 23) so

$$J \approx -(((d\ln J/dT)dT/dt)/V)\ln(N_s/N_o).$$

This equation shows that only a temperature at which a percentage of drops are left can be estimated from nucleation theory. This temperature is defined at the point where 50% of the drops have exploded (refs. 5 and 23), so that

$$J \approx .693\ (((d\ln J/dT)dT/dt)/V) \qquad 105.$$

The slope of the lnJ vs. T curve is determined by solving equations 83a and 90 for a range of nucleation rates, and then determining the rate corresponding to the given experimental conditions (i.e., V and dT/dt). The temperature corresponding to this rate can then be estimated from the tabulated results of the numerical solution.

For numerical analysis it is convenient to write equations 83a and 90 in the following form:

$$J = C \exp(-W/kT) \qquad 106.$$

The values of C and W for equations 83a and 90 are the following:

1) for equation 83a,

$$C = (N_a^{2/3}+N_b^{2/3}) \left[\left(\frac{\Delta_a (P''-P_o)^2}{m_a^{\frac{1}{2}}}\right)\frac{P''_a}{P''} + \left(\frac{16\eta\sigma_b^2}{m_b^{\frac{1}{2}}}\right)\frac{P''_b}{P''}\right] \frac{1}{(\pi^3 128 B\sigma_b^3)^{\frac{1}{2}}} \qquad 107a;$$

$$W = \frac{16\eta\sigma_b^3}{3(P''-P_o)^2} \qquad 107b;$$

$$\Delta_a = 4\pi\,(3MW_a/(4\pi\rho_a N_o))^{2/3} \qquad 107c$$

2) for equation 90,

$$C = N_b \left(\frac{2\sigma_b}{\eta\, m_b B}\right)^{\frac{1}{2}} \qquad 108a;$$

$$W = \frac{16\pi\sigma_b^3}{3(P''_b-P_o)^2} \qquad 108b.$$

Equation 106 can be solved for T to give

$$T = \frac{-W}{k(\ln(J/C))} \qquad 109.$$

Expressing P in atm, ρ in g/cm^3, m_a in g, σ in dyne/cm, and T in deg K, equations 107 and 108 can be re-written as follows (where $N_a = \rho_a N_o/MW_a$, $N_b = \rho N_o/MW_b$, $m_a = MW_a/N_o$ and $m_b = MW_b/N_o$):

1) equation 107,

$$C = 8.786\times10^{25}((\rho_a/MW_a)^{2/3}+(\rho_b/MW_b)^{2/3})(A+B1)/(B\sigma_b^3)^{\frac{1}{2}} \qquad 110a$$

$$A = \left(\frac{1.03\times10^{12}(P''-P_o)^2\Delta_a}{MW_a^{\frac{1}{2}}}\right)\frac{P''_a}{P''} \qquad 110b$$

$$B1 = \left(\frac{50.265\ \sigma_b^2}{MW_b^{\frac{1}{2}}}\right)\frac{P''_b}{P''} \qquad 110c$$

$$W = \frac{1.632\times10^{-11}\ \sigma_b^3}{(P''-P_o)^2} \qquad 110d;$$

2) equation 108,

$$C = 3.73\times10^{35}\left(\frac{\rho_b^2\sigma_b^2}{MW_b^3 B}\right)^{\frac{1}{2}} \qquad 111a$$

$$W = \frac{1.632\times10^{-11}\ \sigma_b^3}{(P''_b-P_o)^2} \qquad 111b.$$

Both (P''_a-P_o) and $(P''-P_o)$ in the above equations are related to the equilibrium vapor pressure by eq. 101.

The terms A and B1 in eq. 110a were grouped according to eqs. 110b and 110c to permit a comparison of their relative orders of magnitude in the numerical solution. It may be noticed that even when A and B1 are the same order of magnitude, setting $\Delta_a = 0$ still has a negligible effect on the nucleation rate.

Equation 109 with equations 110 or 111 was solved by what may be called a modified "binary chop" method (ref. 24). In this method a temperature is assumed and the right hand side of eq. 109 is evaluated at intervals of 10C until a change of sign occurs. The increment is then reduced by an order of magnitude and the right hand side re-calculated at intervals of-1C until another

sign change occurs, and then at intervals of +.1C, etc. Admittedly this method is one of the most unsophisticated and slowly converging root finding algorithms available, at least compared to the secant method or reguli-falsi method (the Newton-Raphson method was ruled out because the required derivative was too tedious to obtain). It is, however, easy to program and always converges.

4. Nucleation in Pure Liquids - Results

The program used to solve for the homogeneous limit of superheat is shown in plate 1. Equations 109 and 111 were programed directly and can be identified in the program listing. (The particular program listed is for a n-decane calculation). The only input required for the program is P''_{ie}, σ_i, ρ_ℓ'', and ρ_ℓ'.

Plates 2 to 7 list the numerical solutions of the nucleation temperatures to the nearest .1C for nucleation rates ranging from $J=1/cm^3$-sec to $J=10^{10}/cm^3$-sec. Listed also are C ($1/cm^3$-sec), σ (dyne/cm), W(dyne-cm), bubble radius R(cm), bubble volume $V(cm^3)$, and number of molecules in the nucleus x.

It is seen that T varies less than 1C per two orders of magnitude change in J, and that there are between 100 and 200 molecules in the critical sized bubble.

A comparison of the experimentally measured temperatures listed in Table I and the numerical solutions given in Plates 2 to 7 shows excellent agreement for all nucleation rates assumed in the theoretical calculations. It is ,nevertheless, useful to estimate what rate corresponds to given experimental conditions.

Injected drop diameters for the pure fuels ranged from about .1mm to 1mm with a median diameter of .5mm being representative. The rate of rise of these drops was about 5cm/sec in the region of explosive boiling (though a precise value is difficult to measure). For a linear gradient of roughly 3C/cm the heating rate is about 15C/sec. The value of $d\ln J/dT$ was determined graphically from a plot of lnJ vs. T (fig. 12 shows such a plot for the special case of decane). As shown in fig. 12 J is well represented as an exponential function of temperature which justifies the approximation of eq. 104. For decane, $d\ln J/dT \approx 6.4$. Similar plots for the other liquids tested would show that $6<d\ln J/dT<8$ which is consistent with values reported in the literature. An average value of $d\ln J/dT \approx 7$ will be used. From eq. 105 the value of J which characterizes the experiments run here for homogeneous nucleation is $J \approx 1.4 \times 10^5$, or more generally $10^4 < J < 10^6$.

Table IV lists the experimentally measured limits of superheat and the theoretical estimates at $J=10^4$ and 10^6. Also included is the experimental result from ref. 13 for water. The large discrepancy between theory and experiment for water has been discussed in the literature (refs. 9 and 13).

5. Nucleation of Fuel Emulsions - Results

Plates 8 and 9 list the program for determining the nucleation temperatures of the emulsions using equations 109 and 110. The same solution method as before was used, and the results of the theoretical predictions at nucleation rates from $J=1$ to $J=10^{10}$ are listed on plates 10 to 14.

For all nucleation rates assumed, agreement between theory and experiment (Table II) is rather good. This agreement was not necessarily expected both because of the experimental problems of measuring emulsion nucleation temperatures and the assumptions used in deriving the theoretical model.

Injected drops had to be greater than about 1mm diameter to avoid complete dissolution of the water. The data listed in Table II were therefore for droplet sizes between 1mm and 2mm diameter. A median size of 1.5mm is assumed with a corresponding volume of .0141 cm^3. The rising drops contained 15% by volume of water. Though the water is ideally considered to be dispersed as tiny droplets in the fuel, this is probably not the case by the time they reach their nucleation temperatures as suggested in the illustration shown in fig. 11. Some coalescence of the water probably occurs so that by the time the injected drop reaches its nucleation temperature, the internal phase may be considered as one large body of water. Whether this is in fact the case is not too important because nucleation at a liquid-liquid interface is being described and whether this interface is between a large body of water and the fuel or the curved surface of a tiny dispersed water drop and the fuel should not make a difference. Hence the dispersed water volume is approximately $.15 \times .0141 = V = 2.12 \times 10^{-3} cm^3$.

The value of $d\ln J/dT$ was graphically determined from the slope of a $\ln J$ vs T curve. Such curves are shown in fig. 12 for all emulsions tested (data obtained from plates 10 to 14). Also included is the data for a water-freon system. It should

be noted that the experiments reported in ref. 4 were performed by injecting pure water drops in a heating medium of freon E9, and not preparing a freon-water emulsion and then injecting a drop of the emulsion into a third fluid as done here. Their results are included here only because the surface and interfacial tensions of freon and water satisfy eq. 80. In any case it is seen that for all the emulsions the value of $d\ln J/dT$ lies between 2.5 and 3.58 with a mean of about 3. This value is to be contrasted to $d\ln J/dT \approx 7$ for homogeneous nucleation in the fuel.

The measured rates of rise of the emulsified drops were around 8cm/sec in a temperature gradient of about 2C/cm so that $dT/dt \approx 16$C/sec. Therefore, from eq. 105

$$J = (.693 \times 3 \times 16)/2.12 \times 10^{-3} = 1.57 \times 10^{4}$$

or,

$$J \approx 10^{4}.$$

Table V lists the esperimental and theoretical predictions (for $J=10^{4}$) of the nucleation temperatures of the emulsions tested. The theoretical predictions are in excellent agreement with the measured temperatures. It must be remembered, though, that only the highest recorded temperatures are listed in Table V. The great majority of rising drops had air bubbles attached to them, and others exploded at lower temperatures probably due to motes or imperfect wetting at the water-fuel interface.

A relative comparison of the theoretical and measured temperatures for both the pure liquids and emulsions examined here is shown graphically in fig. 14. The good agreement of both

homogeneous nucleation (already well established) of the pure liquids and the assumed mechanism of droplet explosions in emulsified fuels is apparent.

The pre-exponential term for nucleation in fuel emulsions is $C \approx 10^{25}$, while for homogeneous nucleation $C \approx 10^{32}$. This reduction is due primarily to considering molecules at the interface rather than molecules within the bulk of the drop as potential nuclei (i.e., $N \rightarrow N^{2/3}$)

The values of A and B1 (defined in equations 110b and 110c) are both approximately the same order of magnitude for all emulsions tested. This might at first imply that including the cross sectional area of an a molecule in the pre-exponential term of eq. 83a is important. However, the large multiplicative factor of 10^{25} in eq. 110a has a damping effect on additive terms of the same order of magnitude. If Δ_a is set equal to zero in eq. 110a, the solution of eq. 109 is not effected and the same temperatures as listed in Table V result. This would lend support to the use of eq. 71 instead of eq. 73 for the general expression describing nucleation at a liquid-liquid interface. However, it would be conceptually difficult to explain how molecules of either liquid could penetrate the interface if $\Delta_a = \Delta_b = 0$. This is so because the assumption was made that the interface is a boundary across which molecules cannot cross unless there is an "opening" for their passage. Of course this is not strictly correct. Nevertheless, for purposes of describing nucleation at a liquid-liquid interface this assumption does lead to results consistent with experimental measurements.

The vapor pressure of water is approximately two orders of magnitude greater than the fuel at the predicted nucleation temperature. The fundamental condition of applicability of eq. 83a is therefore satisfied. Even for a decane-water emulsion where $P''_a \approx 28$atm and $P''_b \approx 4$atm, the predicted temperatures are in quite good agreement with the highest measured explosion temperature . However, just how much more volatile one liquid must be than another for eqs. 66 or 67 to be valid is an open question at this time. The results presented appear to be valid when there is at least a one order of magnitude difference in vapor pressure.

6. Application to Emulsified Fuel Combustion

Disruptive burning of emulsified fuels is well estabilshed in the literature. The cause of this phenomenon is here attributed to nucleation at the internal phase (water) -fuel interface. Whether droplet boiling will or will not occur in a given physical situation is determined primarily by the surface tension of the fuel and the vapor pressure of the water. The addition of an emulsifying agent to the fuel during emulsion preparation changes the mechanism of nucleation from bubble growth between the interface - a lens shaped bubble - to spherical bubble growth tangent to the interface and surrounded by the fuel (fig.3d). Because of this it is not necessary to know a specific value of the interfacial tension of the two liquids composing the

emulsion. The following proportionality based on eq. 83a can then be written:

$$T_s \sim \frac{\sigma_b^3}{(P_a'' + P_b'' - P_o)^2} \qquad 112.$$

To determine whether a particular emulsion will burn disruptively or not, it is necessary to know only whether T_s is greater or less than the boiling point of the fuel at the ambient pressure, P_o. The steady state temperature of a burning pure fuel droplet is not exactly its boiling temperature but is slightly less. This is because the fuel mass fraction at the droplet surface is not exactly 1 but is slightly less due to the presence of the products of combustion (i.e., the vapor pressure of the fuel is not its equilibrium vapor pressure). Nevertheless, in most cases the actual droplet temperature is usually only a few degrees less than its saturation temperature.

The heating period in droplet burning (ref. 25) provides evidence that disruptive burning or fragmentation of the primary fuel droplet will occur only within the first 10% to 20% of the total burning time. The main question is still whether the nucleation temperature (T_s) is greater or less than the steady state droplet burning temperature.

Tables II and V show that for decane, dodecane, and tetradecane emulsions no explosive boiling will occur during combustion because $T_s > T_b$ (boiling temperature) for these emulsions. For a hexadecane-water emulsion disruptive burning should occur because $T_s < T_b$ (i.e., 269.7 < 287.5).

Nucleation temperature predictions for other than water-fuel emulsions stabilized by an emulsifying agent are straightforward. One only has to subsitute the appropriate properties of the internal phase and burning fuel into the computer program listed on plates 8 and 9 to estimate a temperature. One need not go to this trouble for the particular case of an emulsion of methanol and three of the four fuels used here. The homogeneous limit of superheat of methanol is 186C (ref. 15). Since a liquid cannot be heated to a temperature higher than its homogeneous nucleation temperature corresponding to the ambient pressure, internal boiling is guaranteed to occur for an emulsion of n-dodecane, tetradecane, and hexadecane. Simply stated, the steady state droplet burning temperatures of these fuels are all higher than the homogeneous nucleation temperature of methanol (for burning at 1 atm). Such an observation leads to the following generalization for the prediction of droplet explosions in the burning of emulsified fuels: Explosive burning, or at the very least internal boiling, will be guaranteed to occur if the steady state burning temperature is greater than the homogeneous nucleation temperature of the internal phase. If this is not the case, the theoretical formulations derived here can be used to determine at what temperature nucleation should be expected.

This study was concerned only with developing a theoretical model for disruptive burning in emulsified fuels and its experimental verification at <u>latr</u>. While information on high pressure nucleation can be obtained from the results presented here,

there is currently no experimental evidence which could be used in support of any subsequent conclusions (except at latm as reported here). Before this work is finally completed an experimental study of nucleation at high pressures (>10atm) will be undertaken.

A detailed discussion of the role of the suspending quartz fiber in inducing explosive burning of emulsified fuels will also be given at some later time. Such a discussion will not require theoretical formulations beyond what already exist in the literature.

V. Conclusions

A theoretical and experimental investigation of the explosive burning phenomenon in emulsified fuel combustion has been undertaken. The approach was that of using nucleation theory to explain the mechanism of droplet explosion in the burning of such fuels. The theoretical model is based on the assumption that a spherical bubble grows at the interface between the fuel and internal dispersed phase, and is surrounded almost completely by the fuel except for an opening large enough to permit molecules of the volatile internal phase to enter the bubble. The bubble grows until a size, known as the critical size, is reached at which the bubble is in a metastable state. Growth beyond the critical size occurs by the addition of a few more molecules and results in a sudden and rapid boiling of the emulsion drop.

No previous observations (to the authors knowledge) have been reported on free burning emulsion drops.

The experimental method reported here attempted to model this configuration by measuring nucleation temperatures of rising emulsion drops in a heavier heated liquid. This technique enables the emulsified fuel drop to be heated to a temperature well in excess of its boiling point. In a free burning emulsion drop, however, the maximum temperature is limited by the boiling point of the fuel.

The conclusions of this investigation are given below.

1) The expression for the nucleation rate at a liquid-liquid interface has the general form,

$$J = C \exp(-W/kT).$$

When $P''_a \gg P''_b$, the following forms of C and W are assumed depending on the surface and interfacial tensions of the two liquids:

1a) $\sigma_{ab} > \sigma_a - \sigma_b$

$$C=(N_a^{2/3}+N_b^{2/3})\left[\left(\frac{16\pi A_a\sigma_a^2+\Delta_a(P''-P_o)^2(1-A_a)}{m_a^{\frac{4}{2}}}\right)\frac{P''_a}{P''}+\left(\frac{16\pi A_b\sigma_b^2+\Delta_b(P''-P_o)^2(1-A_b)}{m_b^{\frac{4}{2}}}\right)\frac{P''_b}{P''}\right]\frac{1}{(\pi^3 128\sigma_a^3F_a)^{\frac{1}{2}}}$$

$$W = \frac{16\pi\sigma_a^3F_a}{3(P''-P_o)^2}$$

$$F_a=(\sigma_a^3(2-3M_a+M_a^3)+\sigma_b^3(2-3M_b+M_b^3))/(4\sigma_a^3)$$

$$M_a=(\sigma_a^2+\sigma_{ab}^2-\sigma_b^2)/(2\sigma_a\sigma_{ab})$$

$$M_b=(\sigma_b^2+\sigma_{ab}^2-\sigma_a^2)/(2\sigma_b\sigma_{ab})$$

$$B=1-(1/3)(1-P_o/P'')$$

$$A_a=(1-M_a)/2$$

$$A_b=(1-M_b)/2$$

$$P''=P''_a+P''_b;$$

1b) $\sigma_a \geq \sigma_b+\sigma_{ab}$

$$C=(N_a^{2/3}+N_b^{2/3})\left[\left(\frac{\Delta_a(P''-P_o)^2}{m_a^{\frac{1}{2}}}\right)\frac{P''_a}{P''}+\left(\frac{16\pi\sigma_b^2}{m_a^{\frac{1}{2}}}\right)\frac{P''_b}{P''}\right]\frac{1}{(\pi^3 128B\sigma_b^3)^{\frac{1}{2}}}$$

$$W=\frac{16\pi\sigma_b^3}{3(P''-P_o)^2};$$

1c) $\sigma_b = \sigma_a+\sigma_{ab}$

$$C=(N_a^{2/3}+N_b^{2/3})\left[\left(\frac{16\pi\sigma_a^2}{m_a^{\frac{1}{2}}}\right)\frac{P''_a}{P''}+\left(\frac{(P''-P_o)^2\Delta_b}{m_b^{\frac{1}{2}}}\right)\frac{P''_b}{P''}\right]\frac{1}{(\pi^3 128B\sigma_a^3)^{\frac{1}{2}}}$$

$$W=\frac{16\pi\sigma_a^3}{3(P''-P_o)^2};$$

and 1d) $\sigma_b > \sigma_a+\sigma_{ab}$

$$C=N_a\left(\frac{2\sigma_a}{\pi m_a B}\right)^{\frac{1}{2}}$$

$$W=\frac{16\pi\sigma_a^3}{3(P''_a-P_o)^2}.$$

2) Setting $\Delta_a=\Delta_b=0$ in the above equations has a negligible

effect on the nucleation rate.

3) For water-fuel emulsions stabilized by an emulsifying agent, the interfacial tension will be very low and condition 2a above will be satisfied. The nucleation rate is then independent of the interfacial tension and depends only on the pure fuel surface tension and vapor pressure of water.

4) Nucleation temperatures of emulsified fuels can be estimated using nucleation theory. These temperatures are well in excess of the boiling points of the internal phase but less than their homogeneous limits of superheat.

5)The frequency of nucleation at the temperatures listed in Table II was very low (being approximately 1 out of 10). The great majority of drops had air bubbles attached to them which expanded on heating. Dissolution of the water occured during droplet ascent and was most pronounced for emulsion droplets less than about .5mm diameter. Nevertheless, this did not effect superheat temperature predictions.

6) The location of bubble formation can be predicted by determining which of equations 76 to 81 is satisfied for the particular components of the emulsion. This supports the conclusions of reference 4.

7) Disruptive burning (i.e., droplet explosions) will occur if the nucleation temperature as calculated using eq. 83a is less than the steady state burning temperature of the emulsion.

8) If the homogeneous limit of superheat of the internal phase in an emulsion is less than the steady state temperature of a burning drop, disruptive burning will occur. This is sure

to be the case for emulsions of methanol and the higher alkanes such as dodecane, tetradecane, and hexadecane.

References

1. Avedisian, T., "Homogeneous Nucleation Theory as Applied to the Droplet Explosion Mechanism in the Burning of Emulsified Fuels," unpublished report, Princeton University, September 1975.

2. Cohen, E.R., "The Accuracy of the Approximations in Classical Nucleation Theory," J. Stat. Phys., 2, 147 (1970).

3. Katz, J.L., H. Saltsburg, and H. Reiss, "Nucleation in Associated Vapors," J. Colloid and Interf. Sci., 21, 560 (1966).

4. Jarvis, T.J., M.D. Donohue, and J.L. Katz, "Bubble Nucleation Mechanisms of Liquid Droplets Superheated in Other Liquids," J. Colloid and Interf. Sci., 50, 359 (1975).

5. Blander, M., and J.L. Katz, "Bubble Nucleation in Liquids," A.I.ChE.J., 21, 833 (1975).

6. Kagan, Yu, "The Kinetics of Boiling of a Pure Liquid," Russ. J. of Phys. Chem., 34, 42 (1960). [illegible], Princeton [illegible].

7. Andres, R.P., "Kinetics of Nucleation in a Single-Component Gas," Ph.D. Thesis, Department of Chemical Engineering, Princeton University (1962).

8. Katz. J.L., and M. Blander, "Condensation and Boiling: Corrections to Homogeneous Nucleation Theory for Nonideal Gases," J. Colloid and Interf. Sci., 42, 496 (1973).

9. Apfel, R.E., "Vapor Cavity Formation in Liquids," Harvard University Acoustics Research Laboratory, Technical Memorandum 62, February 1970.

10. Katz, J.L., "The Critical Supersaturations Predicted by Nucleation Theory," J.Stat. Phys., 2, 137 (1970).

11. Eberhart, J.G., W. Kremsner, and M. Blander, "Metastability Limits of Superheated Liquids: Bubble Nucleation Temperatures of Hydrocarbons and Their Mixtures," J. Colloid and Interf. Sci., 50, 369 (1975).

12. Batchelor, G.K., An Introduction to Fluid Dynamics, Cambridge University Press, New York (1970).

13. Apfel, R.E., "Water Superheated to 279.5C at Atmospheric Pressure," Nature Phys. Sci., 238, 63 (1972).

14. Dryer, F.L., "Fundamental Concepts on the Use of Emulsions as Fuels," Report No. 1224, Department of Aerospace and Mechanical Sciences, Princeton University (1975).

15. Eberhart, J.G., E.J. Hathaway, and M. Blander, "The Limit of Superheat of Methanol and Ethanol," J. Colloid and Interf. Sci., 44, 389 (1973).

16. Jasper, J.J., J. Phys. Chem. Ref. Data., 1, 841 (1972).

17. Volyak, L.D., Dokl. Akad. Nauk SSSR., 74, 307 (1950).

18. Kudchadker, A.P., G.H. Alani, and B.J. Zwolinski, "Critical Constants of Organic Substances," J. Chem. Rev., 68, 659 (1968).

19. Donahue, D.J., and F.E. Bartell, "The Boundary Tension at Water-Organic Liquid Interfaces," J. Phys. Chem., 56, 480 (1952).

20. Jennings, H.Y., "The Effect of Temperature and Pressure on the Interfacial Tension of Benzene-Water and Normal Decane-Water," J. Colloid and Interf. Sci., 24, 323 (1967).

21. Fowkes, F.L., "Attractive Forces at Interfaces," Ind. and Engr. Chem., 56, 40 (1964).

22. Adam, N.K., The Physics and Chemistry of Surfaces, Third

Edition, Oxford University Press, New York (1941).

23. Renner, T.A., G.H. Kucera, and M. Blander, "Explosive Boiling in Light Hydrocarbons and Their Mixtures," J. Colloid and Interf. Sci., 52, 391 (1975).

24. Acton, F.S., Numerical Methods that Work, Harper and Row, New York (1970).

25. Law, C.K., "Unsteady Droplet Combustion with Droplet Heating," Comb. and Flame, 26, 17 (1976).

26. Dickinson, E., "The Influence of Chain Length on the Surface Tension of Oligomeric Mixtures," J. Colloid and Interf. Sci., 53, 467 (1975).

27. Blander, M., D. Hengstenberg, and J.L. Katz, "Bubble Nucleation in n-Pentane, n-Hexane, Pentane+Hexadecane Mixtures, and Water," J. Phys. Chem., 75, 613 (1971).

Table I

Measured Limits of Superheat of Pure Hydrocarbons

Liquid	MW	T_b(C)	T_s(C)	T_c(C)	T_s/T_c(K/K)
n-Pentane	72.1	36.1	147.	196.5	.895
n-Hexane	86.2	68.7	182.	234.2	.898
Benzene	78.1	80.1	225.3	288.9	.886
n-Octane	114.2	125.6	241.7	295.6	.902
n-Decane	142.3	174.1	282.8	344.3	.904

Key:

MW - molecular weight
T_b - boiling point at latm
T_s - measured nucleation temperature
T_c - critical temperature

Table II

Measured Nucleation Temperatures of Water-Fuel Emulsions
83% fuel, 15% water, 2% emulsifying agent

Fuel	MW_f	T_{bf}(C)	T_s (C)	T_{cf}(C)	T_s/T_{cf}(K/K)
n-Decane	142.3	174.1	228.	344.3	.812
n-Dodecane	170.3	216.2	250.	385.1	.795
n-Tetradecane	198.4	252.5	259.	421.	.767
n-Hexadecane	226.4	287.5	263.	444.	.748
Freon-E9	1614.3	290.	228.[a]	363.	.789

Key:

MW_f-molecular weight of fuel

T_{bf}-boiling point of fuel at 1atm

T_s- nucleation temperature

T_{cf}-critical temperature of fuel

[a] data from reference 4

Table IV

Homogeneous Nucleation:

Comparison of Theory and Experiment

Liquid	T_b	T_{sm}	T_{sc} $J=10^4$	T_{sc} $J=10^6$	$T_{sm}-T_{sc}$
n-Pentane	36.1	147.	146.1	146.7	.3
n-Hexane	68.7	182.	183.4	184.1	-2.1
Benzene	80.1	225.3	228.9	229.8	-4.5
n-Octane	125.6	241.7	238.8	239.5	2.2
n-Decane	174.1	282.8	281.9	282.6	.2
Water	100	279.5[a]	305.4	306.3	-26.8

Key:

T_b-boiling point at 1atm

T_{sm}-measured nucleation temperature

T_{sc}-calculated nucleation temperature using eq. 90

[a]data from reference 13

Table V

Nucleation in Emulsified Fuels:

Comparison of Theory and Experiment

Emulsion	T_{bf}	T_{sm}	T_{sc}^{a}	$T_{sm}-T_{sc}$
Decane-Water	174.1	228.	230.8	-2.8
Dodecane-Water	216.2	250.	252.5	-2.5
Tetradecane-Water	252.2	259.	262.2	-3.2
Hexadecane-Water	287.5	263.	269.7	-6.7
Benzene - Water	353.1	205	212	-7.5
Freon E9-Water	290.	228[b]	231.7[c]	-3.7

Key:

T_{bf}-fuel boiling point at 1atm

T_{sm}-measured nucleation temperature

T_{sc}-calculated nucleation temperature using eq. 83a

[a] $J=10^{4}$

[b] data from reference 4

[c] $J=10^{2}$

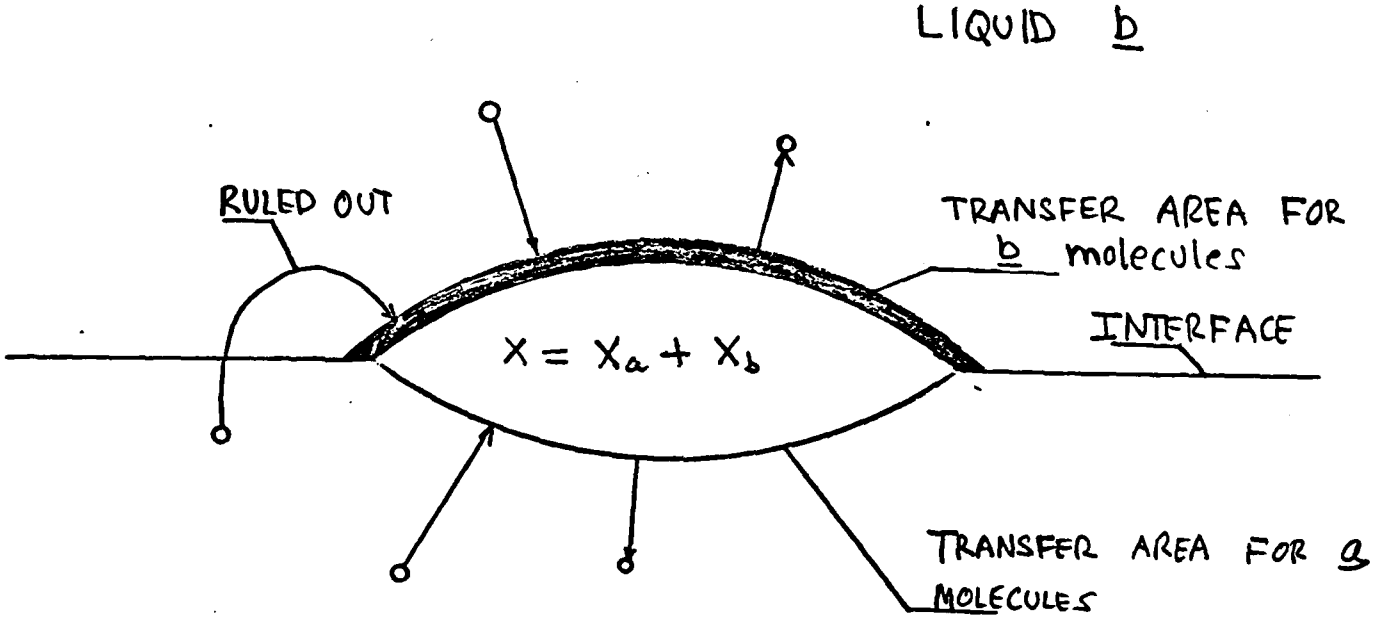

FIG. 1

TRANSFER AREAS FOR BUBBLE GROWTH AT A LIQUID - LIQUID INTERFACE

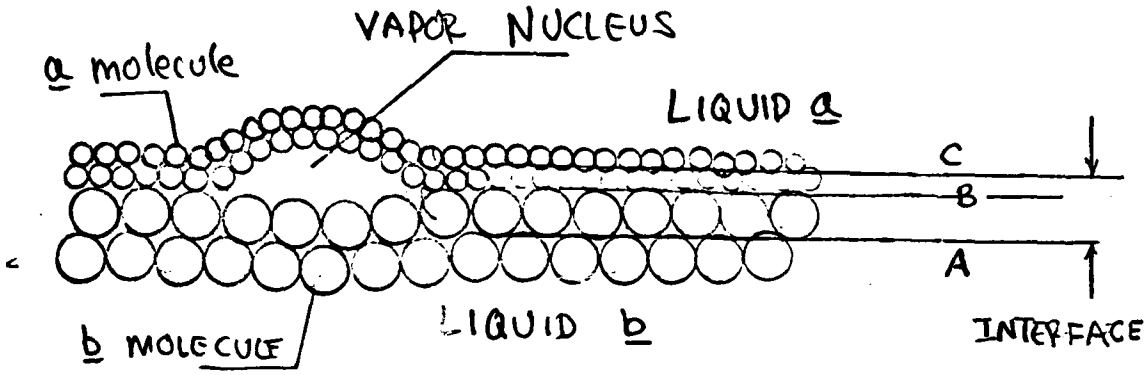

FIG. 2

SCHEMATIC DIAGRAM OF INTERFACIAL REGION BETWEEN TWO IMMISCIBLE LIQUIDS

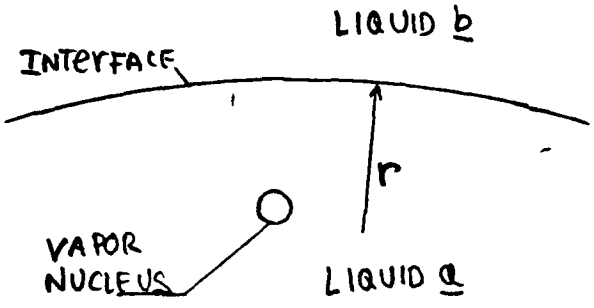

FIG 3a

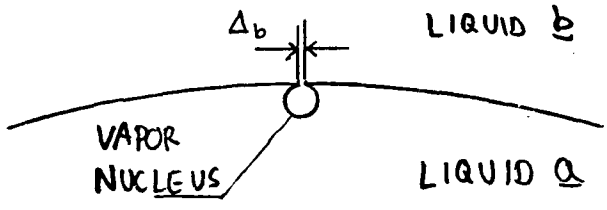

FIG. 3 b

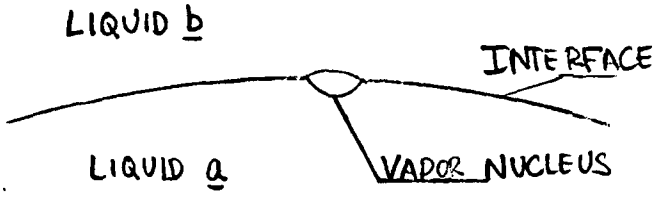

FIG. 3c

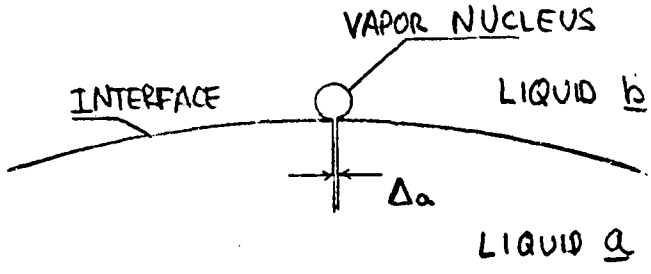

FIG. 3d

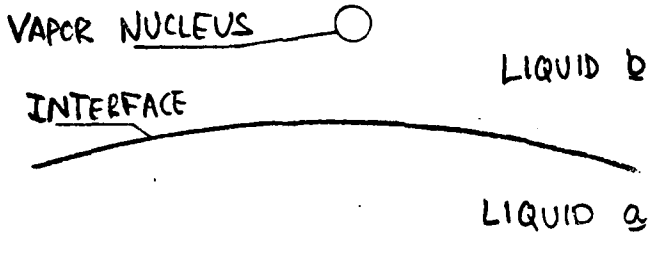

FIG 3e

FIG. 3

POSSIBLE LOCATIONS OF BUBBLE GROWTH AT A LIQUID–LIQUID INTERFACE

AD-A132 177 NUCLEATION AT A LIQUID-LIQUID INTERFACE AND EXPLODING DROPS IN EMULSIFIED FUEL COMBUSTION(U) PRINCETON UNIV N J DEPT OF AEROSPACE AND MECHANICAL SCIENCES. 2/2

UNCLASSIFIED C T AVEDISIAN JUL 76 PUAMS-1315 F/G 21/2 NL

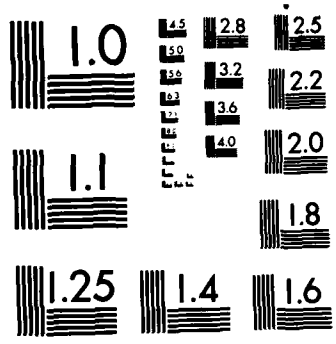

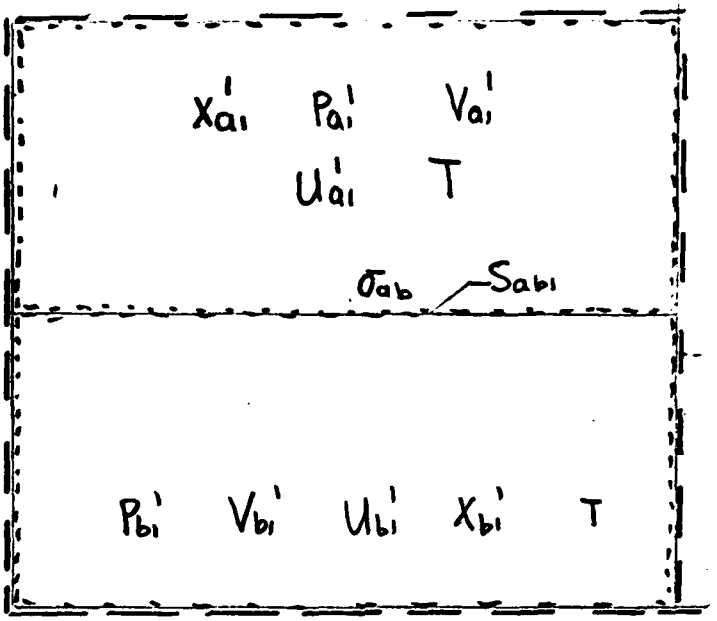

FIG. 4a

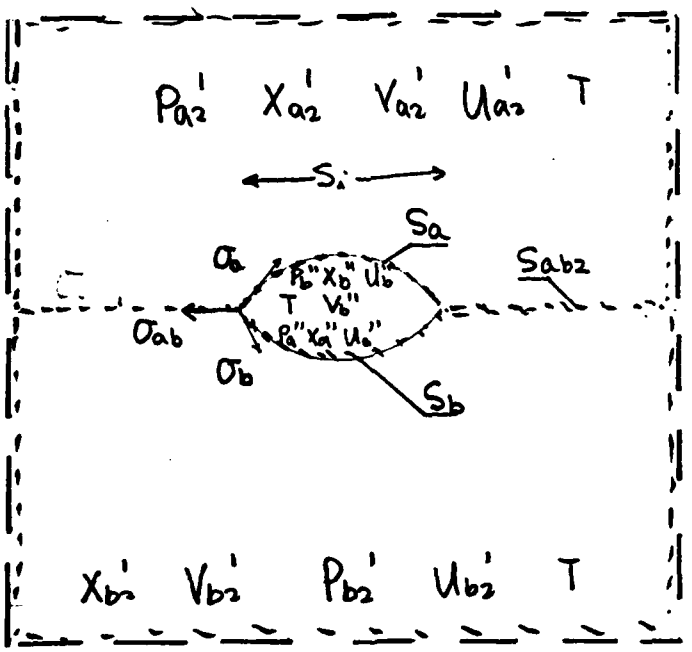

FIG. 4b

— — — — Total system boundary

- - - - - - - - Sub-system boundary

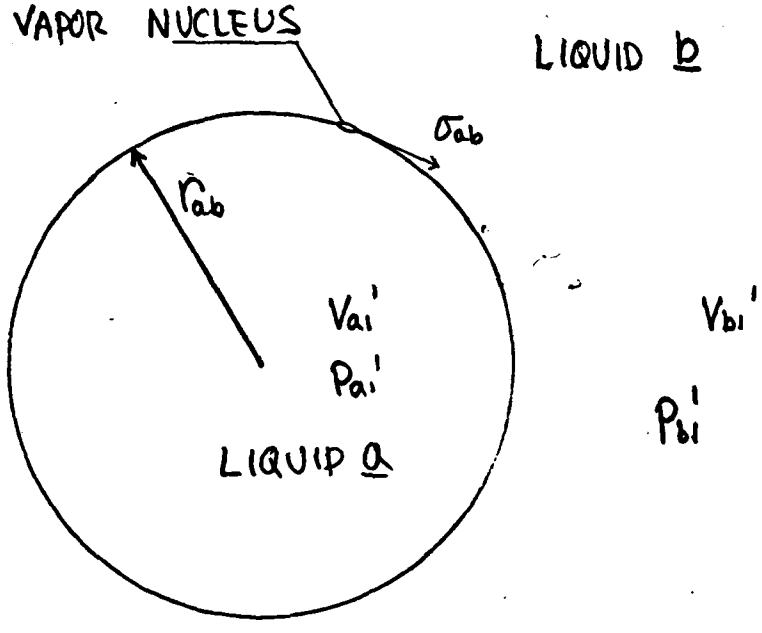

FIG. 5
ILLUSTRATION OF A DROP OF LIQUID a IN A LARGE MASS OF LIQUID b

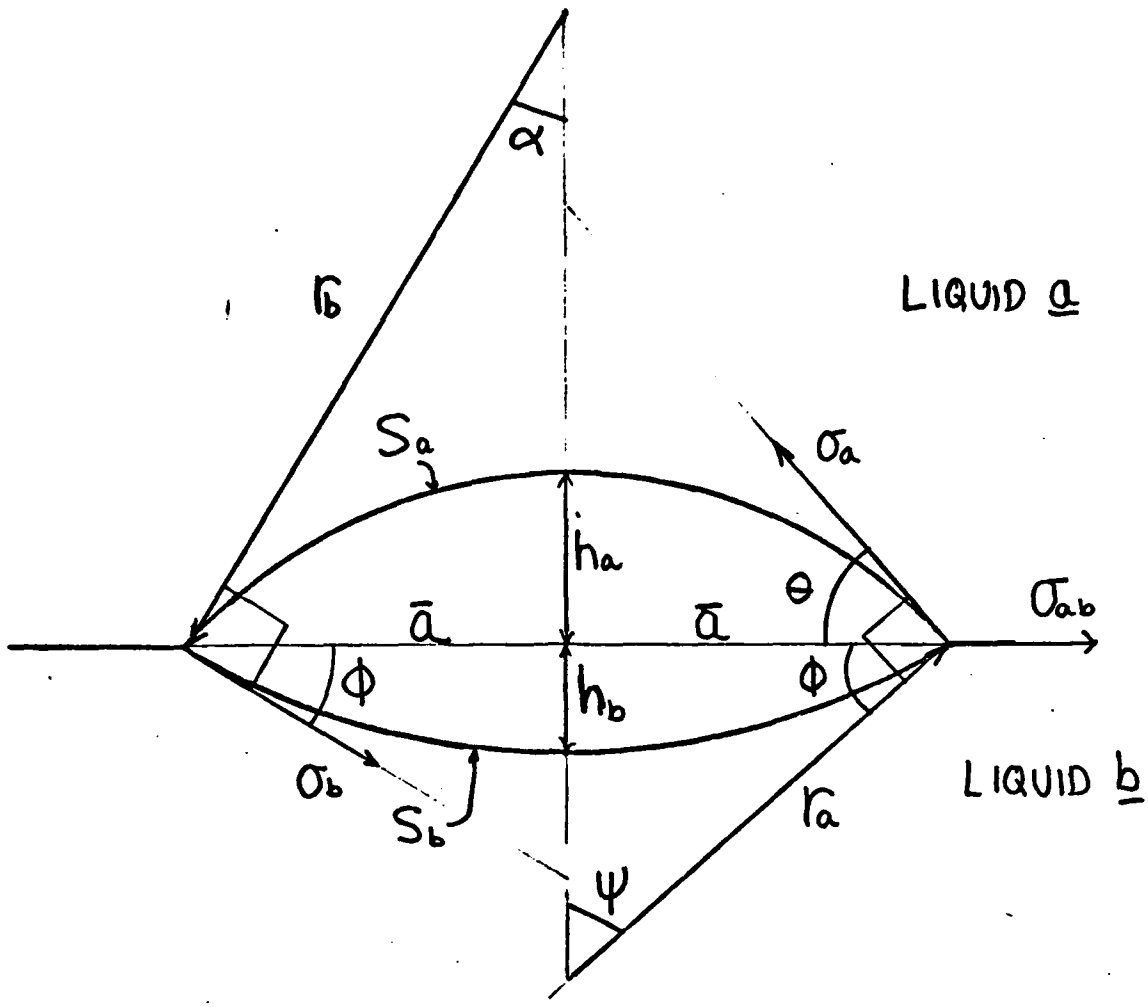

FIG. 6a
GEOMETRY OF A VAPOR LENS

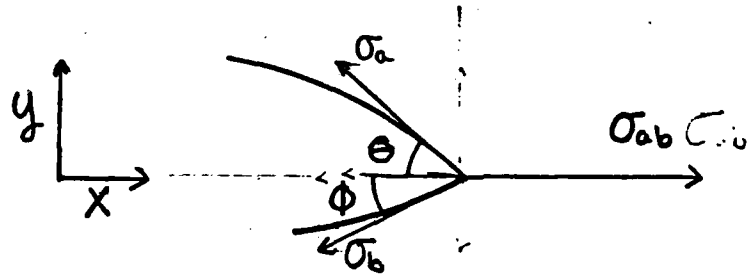

FIG 6b.
FORCE BALANCE AT BUBBLE EDGE

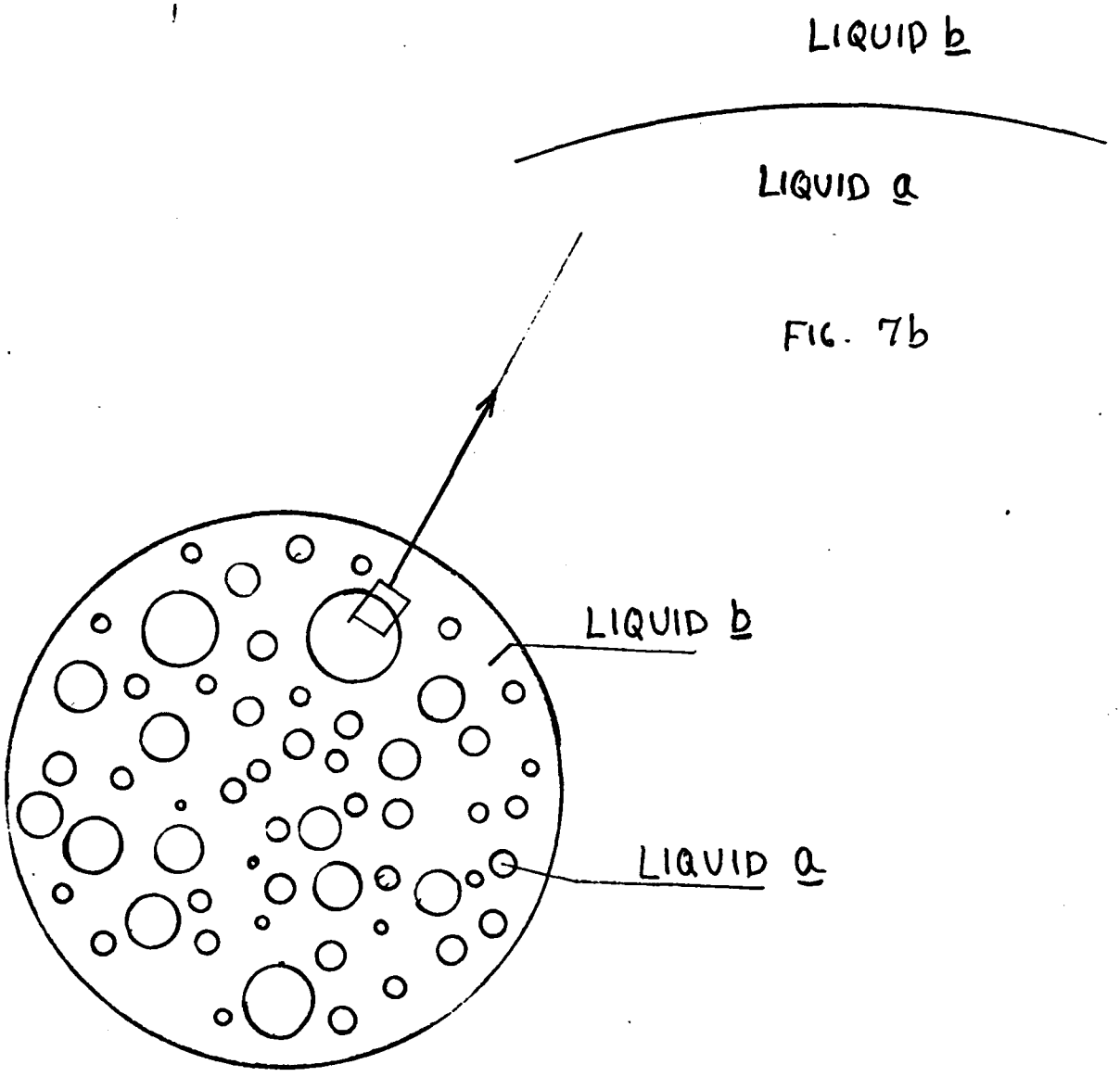

FIG. 7b

FIG 7a

FIG. 7

SCHEMATIC ILLUSTRATION OF AN EMULSION

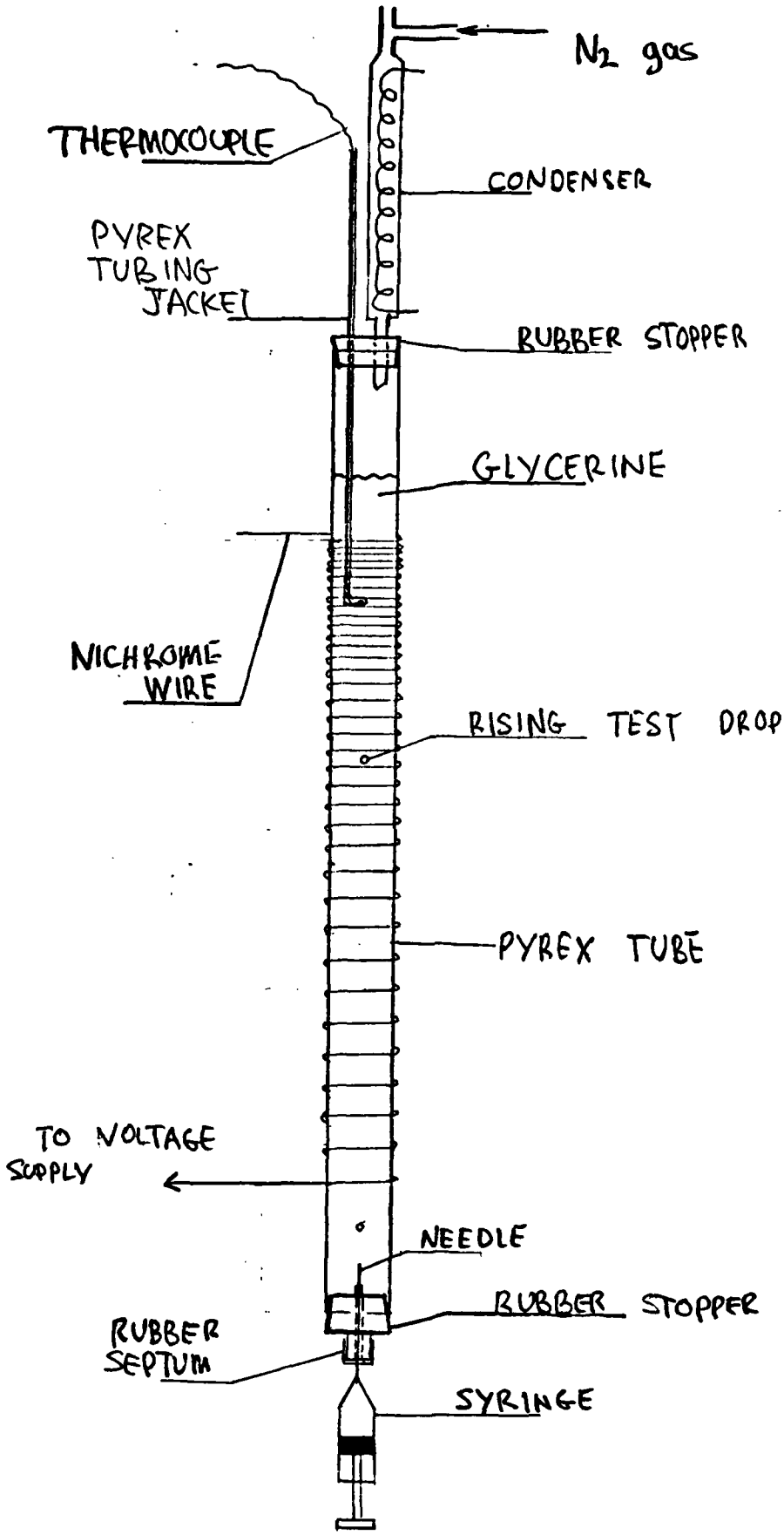

FIG 8
SCHEMATIC OF EXPERIMENTAL APPARATUS

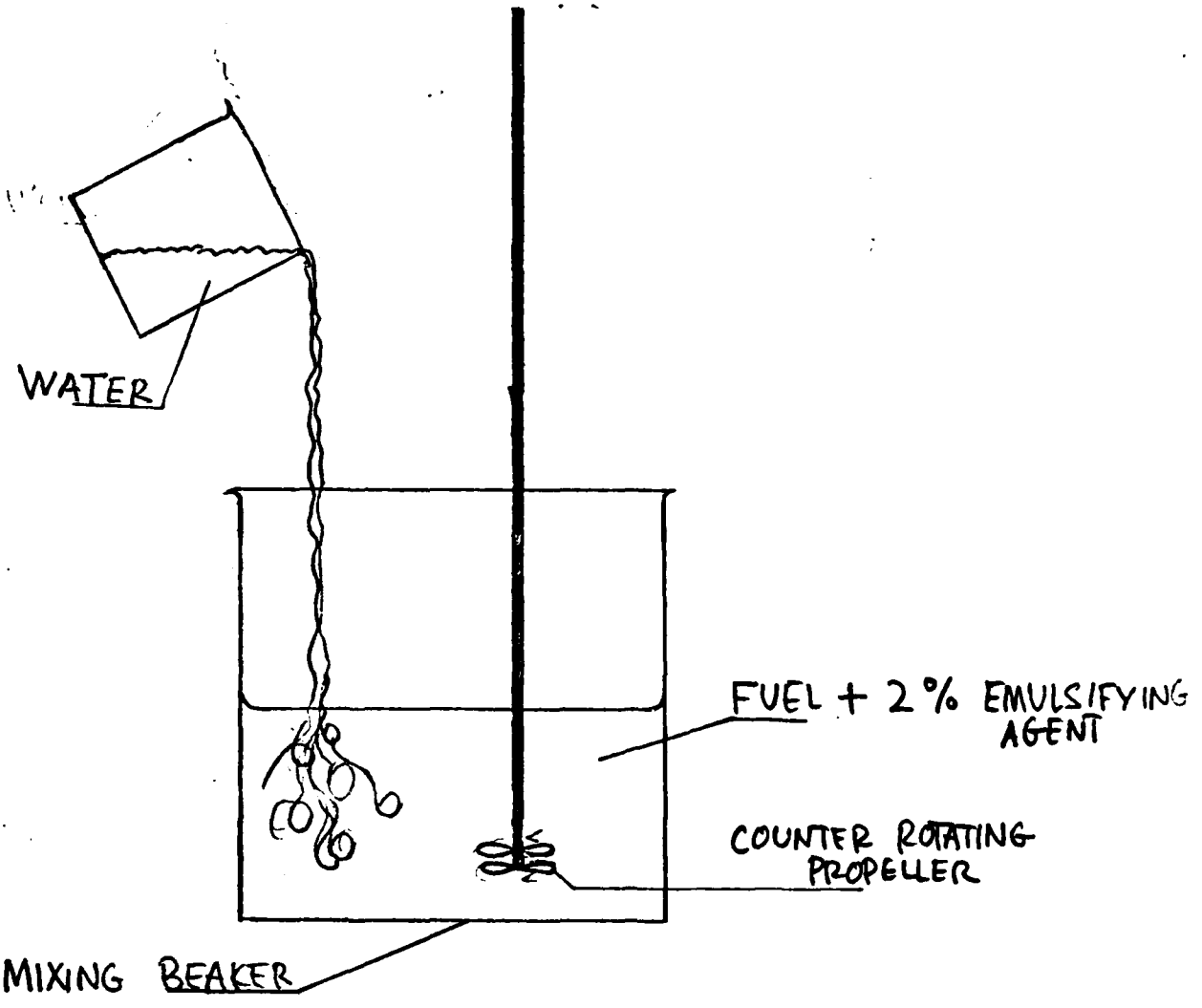

FIG. 9
METHOD OF EMULSION PREPARATION

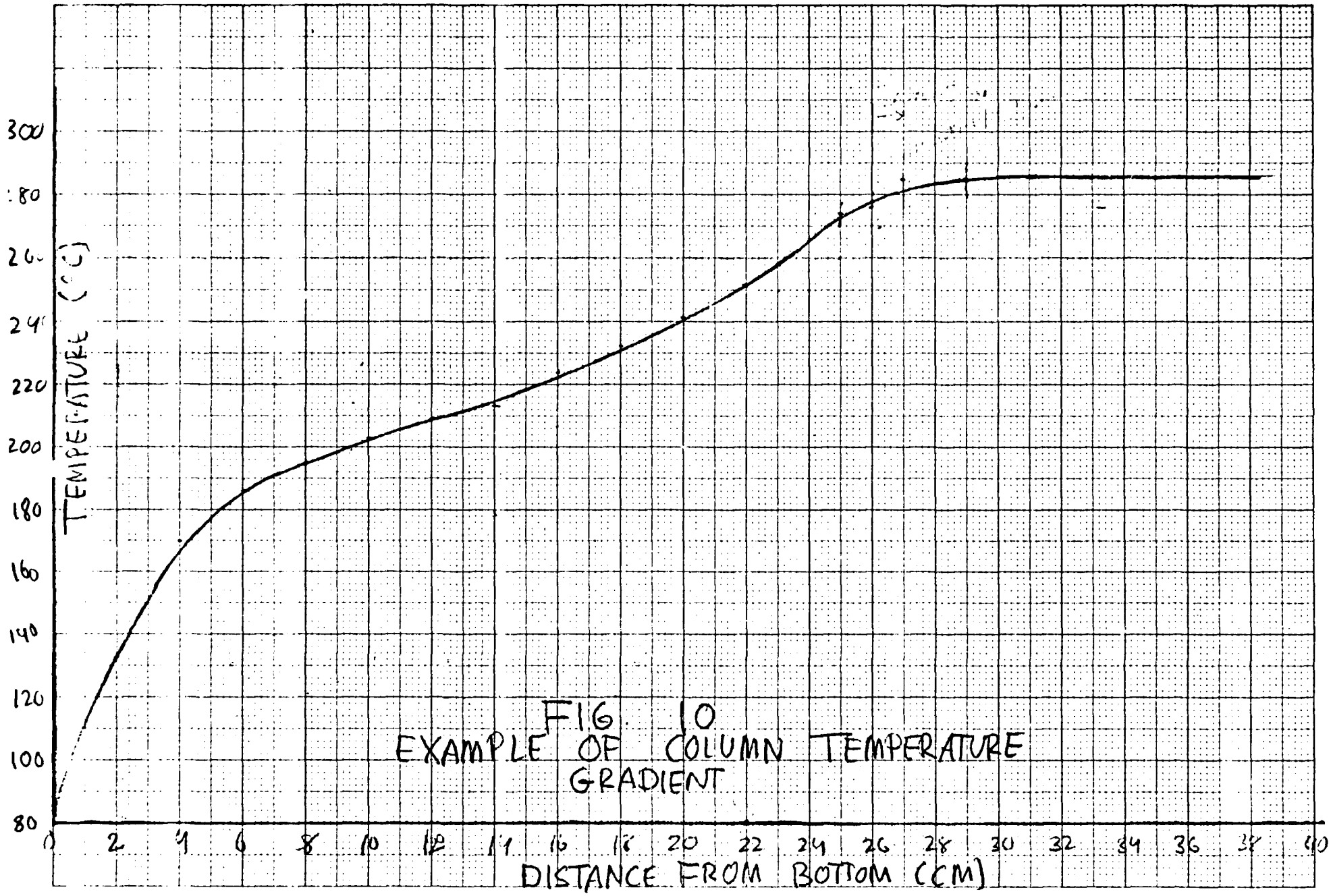

FIG. 10
EXAMPLE OF COLUMN TEMPERATURE GRADIENT

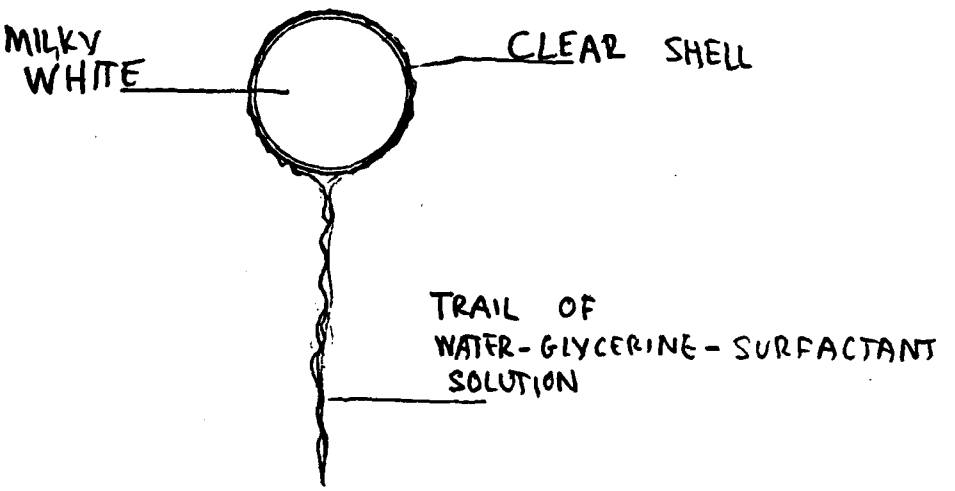

FIG. 11a
EMULSION DROP DURING INITIAL STAGES OF ASCENT

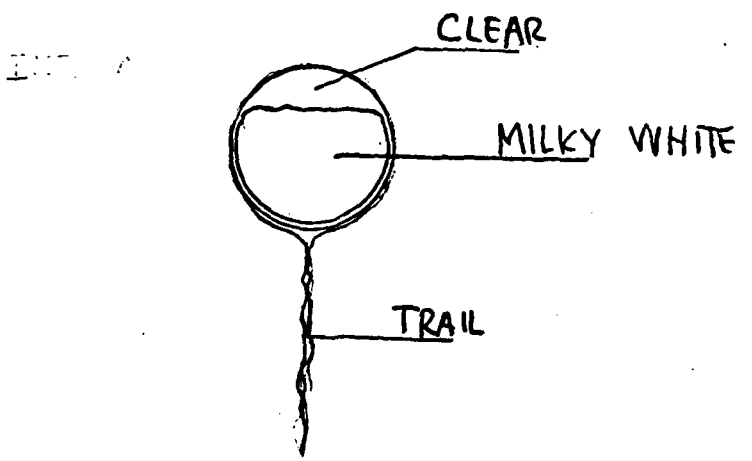

FIG. 11b
DROPLET AT SOME LATER TIME

SOME VISUAL OBSERVATIONS OF WATER-FUEL EMULSIONS RISING IN GLYCERINE

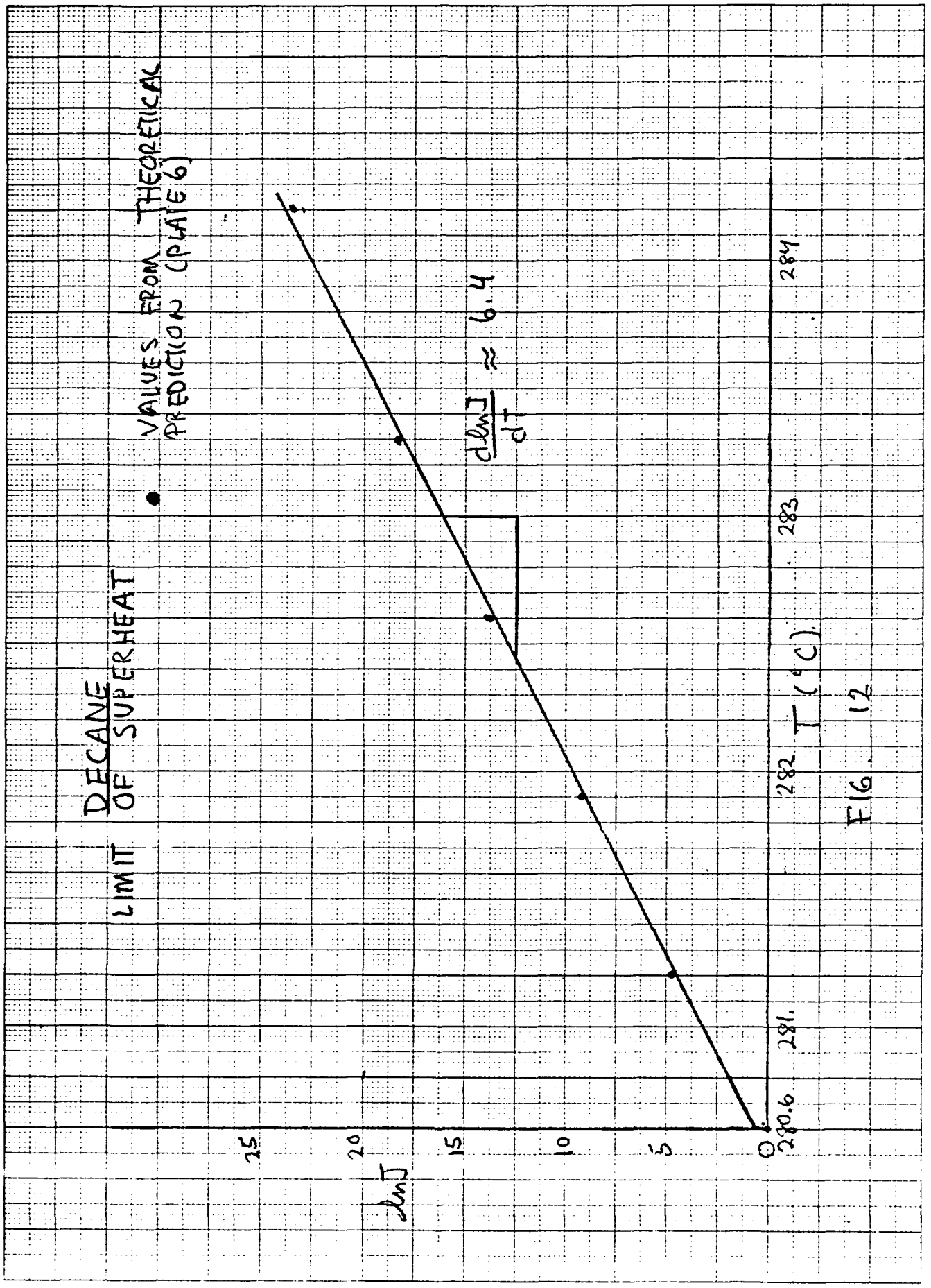

FIG. 12

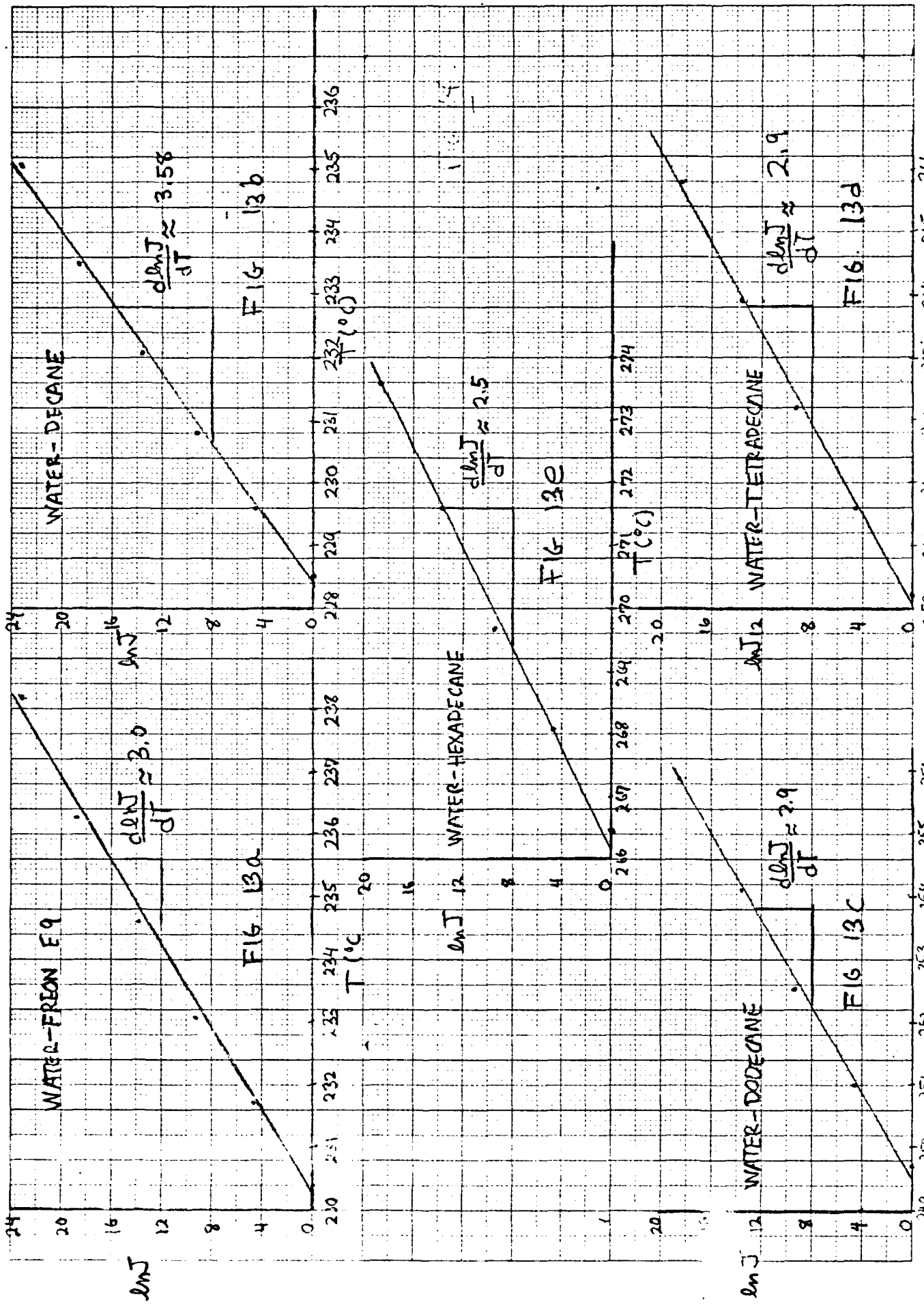

FIG 13

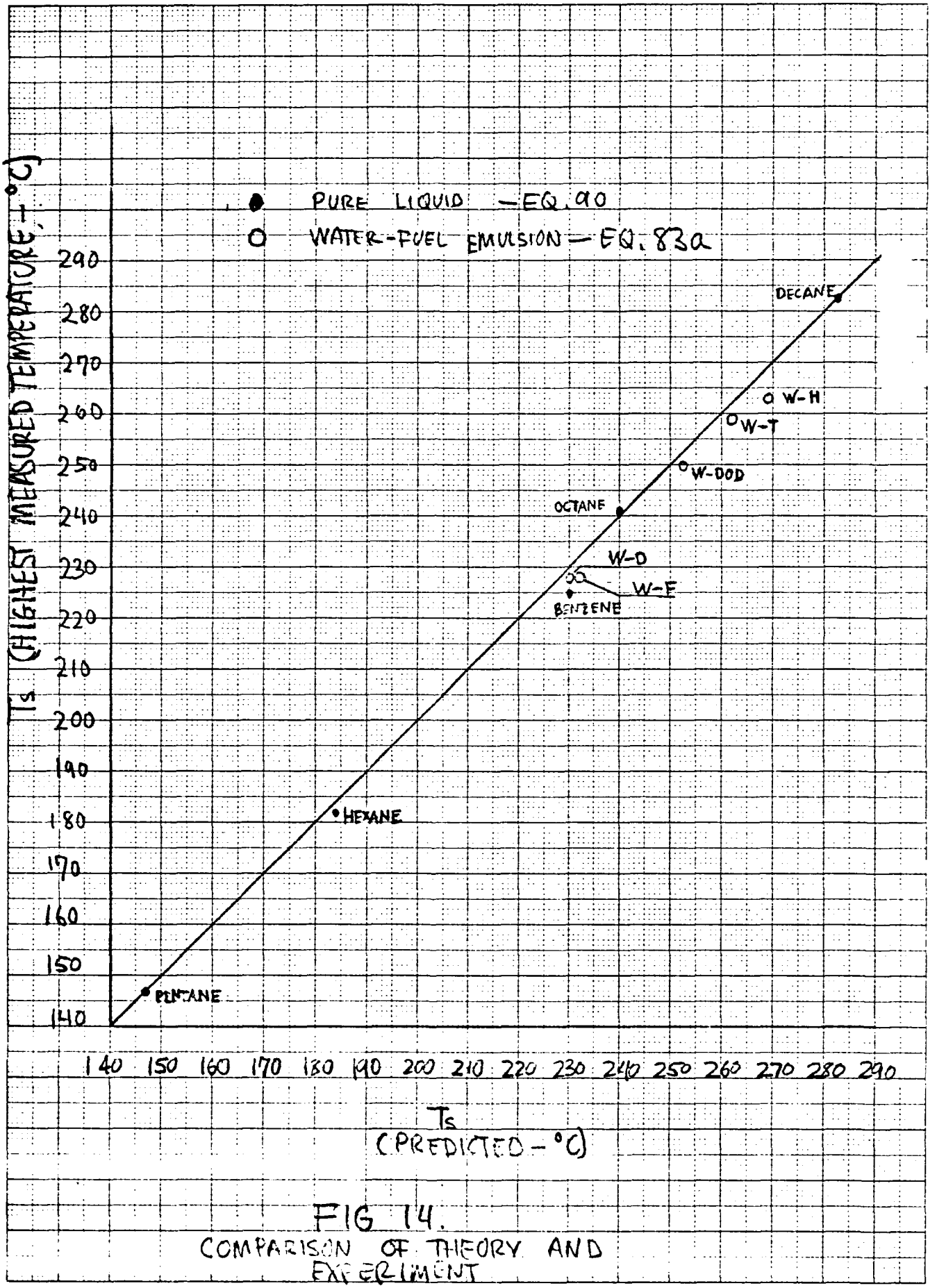

FIG 14.
COMPARISON OF THEORY AND EXPERIMENT

Appendix I

Constants for Equation 93:

$$\sigma = \sigma_o (1 - T/T_c)^n$$

Liquid	σ_o	n	T_c	Reference
Decane	59.37	1.38	617.4	15
Hexadecane	55.2	1.33	717.	26
Hexane	52.4	1.22	507.4	27
Octane	55.72	1.30	568.8	15
Pentane	53.4	1.23	469.4	26
Tetradecane	54.9	1.32	694.	26
Freon E9	37.41	1.22	636.	4

Benzene: $\sigma = 80.877 - .212T + 1.21836 \times 10^{-4} T^2$

Dodecane: $\sigma = 58.75 - .13354T + 6.726 \times 10^{-5} T^2$

Water: $\sigma = 135.547 - .377T + 1.081 \times 10^{-3} T^2 - 2.197 \times 10^{-6} T^3 + 1.424 \times 10^{-9} T^4$

Units: σ - dynes/cm

T - degrees Kelvin

Appendix II

Vapor Pressure as a Function of Temperature

Benzene: $P=\exp(9.3-1.575\times10^{3}/T-1.526\times10^{6}/T^{2}+5.045\times10^{8}/T^{3}-6.295\times10^{10}/T^{4})$

Decane: $P=\exp(8.130-1.406\times10^{3}/T-1.29\times10^{6}/T^{2}+1.33\times10^{8}/T^{3})$

Dodecane: $P=\exp(7.035-321.3/T-1.97\times10^{6}/T^{2}+2.129\times10^{8}/T^{3})$

Hexadecane: $P=10^{(-3366.1/T+8.96)}/760$ *

Hexane: $P=\exp(13.971-8.655\times10^{3}/T+2.589\times10^{6}/T^{2}-5.449\times10^{8}/T^{3}+3.86\times10^{10}/T^{4})$

Octane: $P=\exp(15.16-1.16\times10^{4}/T+4.31\times10^{6}/T^{2}-1.06\times10^{9}/T^{3}+8.871\times10^{10}/T^{4})$

Pentane: $P=\exp(13.56-7.223\times10^{3}/T+1.8\times10^{6}/T^{2}-3.36\times10^{8}/T^{3}+2.11\times10^{10}/T^{4})$

Tetradecane: $P=10^{(-3.004.375/T+8.629)}/760$ *

Freon E9: $P=\exp(24.76-1.755\times10^{4}+2.039\times10^{6}/T^{2})$

Water: $P=\exp(12.409-4.626\times10^{3}/T+1.121\times10^{5}/T^{2}-4.272\times10^{7}/T^{3})$

* equation obtained from CRC Tables

Units: P - atmospheres

T - degrees Kelvin

PLATE I

```
V G LEVEL  21          MAIN          DATE = 76177          13/26/13

      DOUBLE PRECISION TL,T,OA,OB,OAB,DLA,DVA,DLB,DVB,PLA,PLB,RATE,PATM
     1,WA,WB,ALPA,ALPB,XA,XB,P,W,V,B,C,F,DLOG,DEXP,DSQRT,A,B1,P,PA,PB,AJ
     1,AV
      WRITE(6,100)
100   FORMAT('1')
      WRITE(6,400)
400   FORMAT(25X,'LIMIT OF SUPERHEAT-DECANE')
      RATE=1.
2      T=400.15
      I=0
      WRITE(6,200) RATE
200   FORMAT(/'          NUCLEATION RATE = ',D10.3)
1     OA=59.37*((1.-T/617.4)**1.38)
      PLA=DEXP(8.129650475-1406.690454/T-1290900.971/(T**2)+133207218./
     1(T**3))
      DLA=.47
      ALPA=.915
      WA=142.287
      PATM=1.0
      AV=6.02296D23
      P=(PLA-PATM)*ALPA+PATM
      B=1.-(1./3.)*(1.-PATM/P)
      W=1.631982043D-11*(OA**3)/((P-PATM)**2)
      C=3.729537943D35*DSQRT((DLA**2)*OA/((WA**3)*B))
      F=-W/(1.38025D-16*DLOG(RATE/C))
      R=2.*OA/((P-PATM)*1.01325D6)
      V=4.18879*(R**3)
      X=P*1.01325D6*V/(1.38025D-16*T)
      TL=T-273.15
      IF(I.EQ.1) GO TO 15
      IF(I.EQ.2) GO TO 20
      IF(P-T)15,15,10
10    T=T+10.
      GO TO 1
15    T=T-1.
      I=1
      IF(F-T)1,1,19
19    T=T+1.
20    T=T+.1
      I=2
      IF(F-T)35,35,1
35    WRITE(6,8)TL,C,OA,PLA,R,V,W,X
8     FORMAT('   T = ',F6.2,'   C = ',D10.3,'   OA = ',F6.3,'   PLA = '
     1,F6.3,'   R = ',D10.3,/16X,'V = ',D10.3,'   W = ',D10.3,'   X = ',
     1P4.0)
25    RATE=RATE*1.D2
      IF(RATE-5.D10)2,2,26
26    STOP
      END
```

PLATE 2

LIMIT OF SUPERHEAT-PENTANE

NUCLEATION RATE = 0.100D 01

T = 144.90 C = 0.653D 33 OA = 3.512 PLA = 14.715 R = 0.544D-06
V = 0.673D-18 W = 0.435D-11 X = 162.

NUCLEATION RATE = 0.100D 03

T = 145.50 C = 0.648D 33 OA = 3.461 PLA = 14.877 R = 0.530D-06
V = 0.623D-18 W = 0.407D-11 X = 152.

NUCLEATION RATE = 0.100D 05

T = 146.10 C = 0.642D 33 OA = 3.411 PLA = 15.042 R = 0.516D-06
V = 0.577D-18 W = 0.381D-11 X = 142.

NUCLEATION RATE = 0.100D 07

T = 146.70 C = 0.636D 33 OA = 3.361 PLA = 15.207 R = 0.503D-06
V = 0.534D-18 W = 0.357D-11 X = 132.

NUCLEATION RATE = 0.100D 09

T = 147.40 C = 0.629D 33 OA = 3.303 PLA = 15.402 R = 0.488D-06
V = 0.488D-18 W = 0.330D-11 X = 122.

NUCLEATION RATE = 0.100D 11

T = 148.10 C = 0.623D 33 OA = 3.244 PLA = 15.599 R = 0.474D-06
V = 0.446D-18 W = 0.305D-11 X = 113.

PLATE 3

LIMIT OF SUPERHEAT-HEXANE

NUCLEATION RATE = 0.100D 01
T = 182.20 C = 0.477D 33 OA = 3.288 PLA = 13.132 R = 0.585D-06
V = 0.837D-18 W = 0.471D-11 X = 153.

NUCLEATION RATE = 0.100D 03
T = 182.80 C = 0.474D 33 OA = 3.242 PLA = 13.267 R = 0.570D-06
V = 0.776D-18 W = 0.442D-11 X = 153.

NUCLEATION RATE = 0.100D 05
T = 183.40 C = 0.470D 33 OA = 3.197 PLA = 13.402 R = 0.556D-06
V = 0.720D-18 W = 0.414D-11 X = 143.

NUCLEATION RATE = 0.100D 07
T = 184.10 C = 0.467D 33 OA = 3.143 PLA = 13.562 R = 0.540D-06
V = 0.659D-18 W = 0.384D-11 X = 132.

NUCLEATION RATE = 0.100D 09
T = 184.80 C = 0.463D 33 OA = 3.090 PLA = 13.723 R = 0.524D-06
V = 0.603D-18 W = 0.355D-11 X = 122.

NUCLEATION RATE = 0.100D 11
T = 185.50 C = 0.459D 33 OA = 3.038 PLA = 13.886 R = 0.509D-05
V = 0.551D-18 W = 0.329D-11 X = 113.

PLATE 4

LIMIT OF SUPERHEAT-BENZENE

NUCLEATION RATE = 0.100D 01

T = 227.30 C = 0.903D 33 OA = 5.114 PLA = 21.837 R = 0.494D-06
V = 0.504D-18 W = 0.522D-11 X = 158.

NUCLEATION RATE = 0.100D 03

T = 228.10 C = 0.893D 33 OA = 5.041 PLA = 22.153 R = 0.482D-06
V = 0.469D-18 W = 0.490D-11 X = 149.

NUCLEATION RATE = 0.100D 05

T = 228.90 C = 0.882D 33 OA = 4.969 PLA = 22.410 R = 0.470D-06
V = 0.436D-18 W = 0.461D-11 X = 139.

NUCLEATION RATE = 0.100D 07

T = 229.80 C = 0.870D 33 OA = 4.888 PLA = 22.703 R = 0.458D-06
V = 0.402D-18 W = 0.429D-11 X = 130.

NUCLEATION RATE = 0.100D 09

T = 230.80 C = 0.856D 33 OA = 4.799 PLA = 23.031 R = 0.444D-06
V = 0.367D-18 W = 0.397D-11 X = 119.

NUCLEATION RATE = 0.100D 11

T = 231.80 C = 0.843D 33 OA = 4.709 PLA = 23.363 R = 0.431D-06
V = 0.335D-18 W = 0.366D-11 X = 110.

CORE USAGE OBJECT CODE= 3064 BYTES,ARRAY AREA= 0 BYTES,TOTAL AR

DIAGNOSTICS NUMBER OF ERRORS= 0, NUMBER OF WARNINGS= 0, NO

COMPILE TIME= 0.08 SEC,EXECUTION TIME= 0.08 SEC, WATFIV - JUL 1973 V

*** WATFIV VERSION 1.4 *** JOB=004 SUPERHEAT BENZENE

PLATE 5

LIMIT OF SUPERHEAT-OCTANE

NUCLEATION RATE = 0.100D 01
T = 237.50 C = 0.291D 33 OA = 2.874 PLA = 10.379 R = 0.661D-06
V = 0.121D-17 W = 0.526D-11 X = 167.

NUCLEATION RATE = 0.100D 03
T = 238.10 C = 0.290D 33 OA = 2.835 PLA = 10.381 R = 0.645D-06
V = 0.112D-17 W = 0.494D-11 X = 156.

NUCLEATION RATE = 0.100D 05
T = 238.80 C = 0.287D 33 OA = 2.791 PLA = 10.500 R = 0.627D-06
V = 0.103D-17 W = 0.460D-11 X = 145.

NUCLEATION RATE = 0.100D 07
T = 239.50 C = 0.285D 33 OA = 2.746 PLA = 10.721 R = 0.609D-06
V = 0.948D-18 W = 0.427D-11 X = 134.

NUCLEATION RATE = 0.100D 09
T = 240.20 C = 0.283D 33 OA = 2.702 PLA = 10.843 R = 0.592D-06
V = 0.870D-18 W = 0.397D-11 X = 124.

NUCLEATION RATE = 0.100D 11
T = 241.00 C = 0.280D 33 OA = 2.651 PLA = 10.983 R = 0.573D-06
V = 0.788D-18 W = 0.364D-11 X = 114.

PLATE 6

LIMIT OF SUPERHEAT-DECANE

NUCLEATION RATE = 0.100D 01

T = 280.60 C = 0.197D 33 OA = 2.581 PLA = 8.706 R = 0.723D-06
V = 0.158D-17 W = 0.565D-11 X = 169.

NUCLEATION RATE = 0.100D 03

T = 281.20 C = 0.196D 33 OA = 2.548 PLA = 8.787 R = 0.706D-06
V = 0.147D-17 W = 0.532D-11 X = 158.

NUCLEATION RATE = 0.100D 05

T = 281.90 C = 0.195D 33 OA = 2.509 PLA = 8.883 R = 0.687D-06
V = 0.136D-17 W = 0.495D-11 X = 147.

NUCLEATION RATE = 0.100D 07

T = 282.60 C = 0.193D 33 OA = 2.470 PLA = 8.980 R = 0.668D-06
V = 0.125D-17 W = 0.461D-11 X = 137.

NUCLEATION RATE = 0.100D 09

T = 283.30 C = 0.192D 33 OA = 2.431 PLA = 9.077 R = 0.649D-06
V = 0.115D-17 W = 0.429D-11 X = 127.

NUCLEATION RATE = 0.100D 11

T = 284.20 C = 0.190D 33 OA = 2.382 PLA = 9.203 R = 0.626D-06
V = 0.103D-17 W = 0.392D-11 X = 115.

PLATE 7

LIMIT OF SUPERHEAT-WATER

NUCLEATION RATE = 0.100D 01
T = 303.70 C = 0.151D 35 OA = 13.675 PLA = 90.345 R = 0.331D-06
V = 0.151D-18 W = 0.626D-11 X = 159.

NUCLEATION RATE = 0.100D 03
T = 304.50 C = 0.149D 35 OA = 13.491 PLA = 91.353 R = 0.323D-06
V = 0.141D-18 W = 0.590D-11 X = 150.

NUCLEATION RATE = 0.100D 05
T = 305.40 C = 0.148D 35 OA = 13.284 PLA = 92.497 R = 0.315D-06
V = 0.131D-18 W = 0.551D-11 X = 140.

NUCLEATION RATE = 0.100D 07
T = 306.30 C = 0.146D 35 OA = 13.078 PLA = 93.652 R = 0.307D-06
V = 0.121D-18 W = 0.515D-11 X = 130.

NUCLEATION RATE = 0.100D 09
T = 307.20 C = 0.144D 35 OA = 12.872 PLA = 94.817 R = 0.299D-06
V = 0.111D-18 W = 0.481D-11 X = 121.

NUCLEATION RATE = 0.100D 11
T = 308.20 C = 0.143D 35 OA = 12.643 PLA = 96.125 R = 0.290D-06
V = 0.102D-18 W = 0.445D-11 X = 112.

PLATE 8

```
FTN IV G LEVEL  21                    MAIN                    DATE = 76177          14/17/22

      DOUBLE PRECISION TL,T,OA,OB,OAB,DLA,DVA,DLB,DVB,PLA,PLB,RATE,PATM
     1,WA,WB,ALPA,ALPB,XA,XB,R,W,V,B,C,F,DLOG,DEXP,DSQRT,A,B1,P,PA,PB,AJ
     1,AV
      WRITE(6,100)
  100 FORMAT('1')
      WRITE(6,400)
  400 FORMAT(30X,'WATER-TETRADECANE'/)
      RATE=1.
    2 T=503.15
      I=0
      WRITE(6,200) RATE
  200 FORMAT(/'                NUCLEATION RATE = ',D10.3)
    1 OB=54.9*((1.-T/694.)**1.32)
      OA=135.547-.377235*T+.0010812*(T**2.)-2.197D-6*(T**3.)+1.424D-9*(
     1T**4.)
      DLA=.514067+.002923*T-4.558D-6*(T**2.)
      DLB=.60
      DVA=DEXP(-24.09765969+.05538578*T-3.1961079D-5*(T**2.))
      DVB=0.0
      PLA=DEXP(12.40918-4626.3369/T+112149.8279/(T**2.)-42723878.31/(T*
     1*3.))
      PLB=(1./760.)*(10.**(-3004.375/T+8.628699))
      WA=18.015
      WB=198.935
      ALPB=.915
      PATM=1.0
      OAB=50.066+.0027247*PATM-.1205*(T-298.15)
      AV=6.02296D23
      ALPA=1.-(DVA/DLA)+.5*((DVA/DLA)**2.)
      PA=(PLA-PATM)*ALPA+PATM
      PB=(PLB-PATM)*ALPB+PATM
      P=PA+PB
      B=1.-(1./3.)*(1.-PATM/P)
      DELA=12.566371*((3.*WA/(12.566371*DLA*AV))**.6667)
      A=1.026675563D12*PA*((P-PATM)**2)*DELA/(P*DSQRT(WA))
      B1=50.26548246*(OB**2)*PB/(P*DSQRT(WB))
      W=1.631982043D-11*(OB**3 )/((P-PATM)**2)
      C=8.786D25*(A+B1)*(1./DSQRT((OB**3)*B))*((DLA/WA)**.667+(DLB/WB)*
     1*.667)
      F=-W/(1.38025D-16*DLOG(RATE/C))
      R=2.*OB/((P-PATM)*1.01325D6)
      V=4.18879*(R**3 )
      XA=PA*1.01325D6*V/(1.38025D-16*T)
      XB=PB*1.01325D6*V/(1.38025D-16*T)
      TL=T-273.15
      IF(I.EQ.1) GO TO 15
      IF(I.EQ.2) GO TO 20
      IF(F-T)15,15,10
   10 T=T+10.
      GO TO 1
   15 T=T-1.0
      I=1
      IF(F-T)1,1,19
   19 T=T+1.
   20 T=T+.1
      I=2
```

PLATE 9

```
IV G LEVEL  21                    MAIN                    DATE = 76177          14/17/22

      IF(F-T) 35,35,1
   35 WRITE(6,8) TL,C,OA,OB,PLA,PLB,R,V,XA,XB,W,A,B1
    8 FORMAT('    T = ',F6.2,'    C = ',D10.3,'    OA = ',F6.3,'    OB = ',
     1F6.3,'    PLA = ',F6.3,/16X,'PLB = ',F6.3,'    R = ',D10.3,'    V = '
     1,D10.3,'    XA = ',F5.0,/16X,'XB = ',F3.0,'    W = ',D10.3,'    A = '
     1,D11.4,'    B1 = ',D11.4)
   25 RATE=RATE*1.D2
      IF(RATE-5.D10) 2,2,26
   26 STOP
      END
```

PLATE 10

WATER-DECANE

NUCLEATION RATE = 0.100D 01
T = 228.50 C = 0.197D 26 OA = 31.222 OB = 5.892 PLA = 26.955
PLB = 3.494 R = 0.403D-06 V = 0.275D-18 XA = 107.
XB = 13. W = 0.401D-11 A = 0.9406D 00 B1 = 0.1609D 02

NUCLEATION RATE = 0.100D 03
T = 229.60 C = 0.196D 26 OA = 30.966 OB = 5.815 PLA = 27.512
PLB = 3.570 R = 0.390D-06 V = 0.248D-18 XA = 98.
XB = 12. W = 0.370D-11 A = 0.9819D 00 B1 = 0.1568D 02

NUCLEATION RATE = 0.100D 05
T = 230.80 C = 0.196D 26 OA = 30.688 OB = 5.731 PLA = 28.129
PLB = 3.655 R = 0.376D-06 V = 0.222D-18 XA = 89.
XB = 11. W = 0.339D-11 A = 0.1029D 01 B1 = 0.1525D 02

NUCLEATION RATE = 0.100D 07
T = 232.10 C = 0.195D 26 OA = 30.386 OB = 5.640 PLA = 28.810
PLB = 3.749 R = 0.361D-06 V = 0.197D-18 XA = 81.
XB = 10. W = 0.307D-11 A = 0.1082D 01 B1 = 0.1479D 02

NUCLEATION RATE = 0.100D 09
T = 233.50 C = 0.195D 26 OA = 30.060 OB = 5.543 PLA = 29.558
PLB = 3.852 R = 0.345D-06 V = 0.173D-18 XA = 73.
XB = 9. W = 0.277D-11 A = 0.1141D 01 B1 = 0.1430D 02

NUCLEATION RATE = 0.100D 11
T = 235.10 C = 0.194D 26 OA = 29.687 OB = 5.433 PLA = 30.430
PLB = 3.972 R = 0.329D-06 V = 0.149D-18 XA = 64.
XB = 8. W = 0.246D-11 A = 0.1213D 01 B1 = 0.1376D 02

PLATE 11

WATER-DODECANE

NUCLEATION RATE = 0.100D 01
T = 249.60 C = 0.955D 25 OA = 26.299 OB = 7.321 PLA = 39.272
PLB = 2.053 R = 0.368D-06 V = 0.208D-18 XA = 112.
XB = 6. W = 0.415D-11 A = 0.1921D 01 B1 = 0.1025D 02

NUCLEATION RATE = 0.100D 03
T = 251.00 C = 0.962D 25 OA = 25.971 OB = 7.232 PLA = 40.219
PLB = 2.111 R = 0.355D-06 V = 0.187D-18 XA = 103.
XB = 5. W = 0.381D-11 A = 0.2019D 01 B1 = 0.1004D 02

NUCLEATION RATE = 0.100D 05
T = 252.50 C = 0.971D 25 OA = 25.619 OB = 7.138 PLA = 41.253
PLB = 2.176 R = 0.341D-06 V = 0.167D-18 XA = 93.
XB = 5. W = 0.349D-11 A = 0.2128D 01 B1 = 0.9828D 01

NUCLEATION RATE = 0.100D 07
T = 254.10 C = 0.981D 25 OA = 25.244 OB = 7.038 PLA = 42.379
PLB = 2.246 R = 0.328D-06 V = 0.147D-18 XA = 85.
XB = 4. W = 0.317D-11 A = 0.2250D 01 B1 = 0.9601D 01

NUCLEATION RATE = 0.100D 09
T = 255.90 C = 0.994D 25 OA = 24.822 OB = 6.925 PLA = 43.673
PLB = 2.327 R = 0.313D-06 V = 0.129D-18 XA = 76.
XB = 4. W = 0.284D-11 A = 0.2394D 01 B1 = 0.9348D 01

NUCLEATION RATE = 0.100D 11
T = 257.90 C = 0.101D 26 OA = 24.353 OB = 6.801 PLA = 45.146
PLB = 2.419 R = 0.298D-06 V = 0.110D-18 XA = 67.
XB = 4. W = 0.252D-11 A = 0.2563D 01 B1 = 0.9070D 01

PLATE 12

WATER-TETRADECANE

NUCLEATION RATE = 0.100D 01

T = 259.20 C = 0.599D 25 OA = 24.048 OB = 8.022 PLA = 46.123
PLB = 1.271 R = 0.353D-06 V = 0.183D-18 XA = 113.
XB = 3. W = 0.418D-11 A = 0.2610D 01 B1 = 0.6235D 01

NUCLEATION RATE = 0.100D 03

T = 260.60 C = 0.612D 25 OA = 23.719 OB = 7.931 PLA = 47.194
PLB = 1.315 R = 0.341D-06 V = 0.166D-18 XA = 104.
XB = 3. W = 0.386D-11 A = 0.2736D 01 B1 = 0.6153D 01

NUCLEATION RATE = 0.100D 05

T = 262.20 C = 0.626D 25 OA = 23.344 OB = 7.826 PLA = 48.440
PLB = 1.367 R = 0.328D-06 V = 0.147D-18 XA = 95.
XB = 3. W = 0.352D-11 A = 0.2887D 01 B1 = 0.6059D 01

NUCLEATION RATE = 0.100D 07

T = 263.90 C = 0.643D 25 OA = 22.945 OB = 7.716 PLA = 49.792
PLB = 1.425 R = 0.314D-06 V = 0.130D-18 XA = 86.
XB = 2. W = 0.320D-11 A = 0.3055D 01 B1 = 0.5960D 01

NUCLEATION RATE = 0.100D 09

T = 265.80 C = 0.664D 25 OA = 22.499 OB = 7.593 PLA = 51.336
PLB = 1.491 R = 0.300D-06 V = 0.114D-18 XA = 76.
XB = 2. W = 0.287D-11 A = 0.3252D 01 B1 = 0.5849D 01

NUCLEATION RATE = 0.100D 11

T = 267.90 C = 0.688D 25 OA = 22.007 OB = 7.457 PLA = 53.084
PLB = 1.567 R = 0.286D-06 V = 0.975D-19 XA = 69.
XB = 2. W = 0.255D-11 A = 0.3483D 01 B1 = 0.5727D 01

PLATE 13

WATER-HEXADECANE

NUCLEATION RATE = 0.100D 01
T = 266.60 C = 0.401D 25 OA = 22.312 OB = 8.604 PLA = 51.997
PLB = 0.690 R = 0.341D-06 V = 0.167D-18 XA = 113.
XB = 2. W = 0.420D-11 A = 0.3287D 01 B1 = 0.3439D 01

NUCLEATION RATE = 0.100D 03
T = 268.10 C = 0.415D 25 OA = 21.960 OB = 8.508 PLA = 53.253
PLB = 0.718 R = 0.330D-06 V = 0.150D-18 XA = 104.
XB = 1. W = 0.388D-11 A = 0.3451D 01 B1 = 0.3411D 01

NUCLEATION RATE = 0.100D 05
T = 269.70 C = 0.431D 25 OA = 21.585 OB = 8.405 PLA = 54.618
PLB = 0.749 R = 0.318D-06 V = 0.135D-18 XA = 95.
XB = 1. W = 0.356D-11 A = 0.3633D 01 B1 = 0.3380D 01

NUCLEATION RATE = 0.100D 07
T = 271.60 C = 0.452D 25 OA = 21.139 OB = 8.283 PLA = 56.274
PLB = 0.788 R = 0.304D-06 V = 0.118D-18 XA = 86.
XB = 1. W = 0.322D-11 A = 0.3861D 01 B1 = 0.3344D 01

NUCLEATION RATE = 0.100D 09
T = 273.60 C = 0.475D 25 OA = 20.671 OB = 8.155 PLA = 58.057
PLB = 0.830 R = 0.291D-06 V = 0.103D-18 XA = 77.
XB = 1. W = 0.289D-11 A = 0.4113D 01 B1 = 0.3305D 01

NUCLEATION RATE = 0.100D 11
T = 275.90 C = 0.503D 25 OA = 20.132 OB = 8.009 PLA = 60.160
PLB = 0.880 R = 0.276D-06 V = 0.982D-19 XA = 68.
XB = 1. W = 0.256D-11 A = 0.4420D 01 B1 = 0.3260D 01

PLATE 14

WATER-FREON-E9

NUCLEATION RATE = 0.100D 01
T = 230.40 C = 0.126D 25 OA = 30.781 OB = 5.517 PLA = 27.922
PLB = 0.125 R = 0.408D-06 V = 0.285D-18 XA = 114.
XB = 1. W = 0.385D-11 A = 0.8998D 00 B1 = 0.2323D 00

NUCLEATION RATE = 0.100D 03
T = 231.70 C = 0.133D 25 OA = 30.479 OB = 5.451 PLA = 28.599
PLB = 0.132 R = 0.394D-06 V = 0.256D-18 XA = 105.
XB = 1. W = 0.354D-11 A = 0.9463D 00 B1 = 0.2298D 00

NUCLEATION RATE = 0.100D 05
T = 233.10 C = 0.141D 25 OA = 30.153 OB = 5.380 PLA = 29.343
PLB = 0.139 R = 0.379D-06 V = 0.228D-18 XA = 95.
XB = 1. W = 0.323D-11 A = 0.9988D 00 B1 = 0.2266D 00

NUCLEATION RATE = 0.100D 07
T = 234.60 C = 0.150D 25 OA = 29.804 OB = 5.304 PLA = 30.155
PLB = 0.147 R = 0.363D-06 V = 0.201D-18 XA = 86.
XB = 1. W = 0.293D-11 A = 0.1058D 01 B1 = 0.2233D 00

NUCLEATION RATE = 0.100D 09
T = 236.30 C = 0.161D 25 OA = 29.408 OB = 5.218 PLA = 31.097
PLB = 0.156 R = 0.346D-06 V = 0.174D-18 XA = 77.
XB = 0. W = 0.262D-11 A = 0.1129D 01 B1 = 0.2198D 00

NUCLEATION RATE = 0.100D 11
T = 238.30 C = 0.176D 25 OA = 28.941 OB = 5.118 PLA = 32.235
PLB = 0.168 R = 0.328D-06 V = 0.147D-18 XA = 67.
XB = 0. W = 0.230D-11 A = 0.1216D 01 B1 = 0.2158D 00

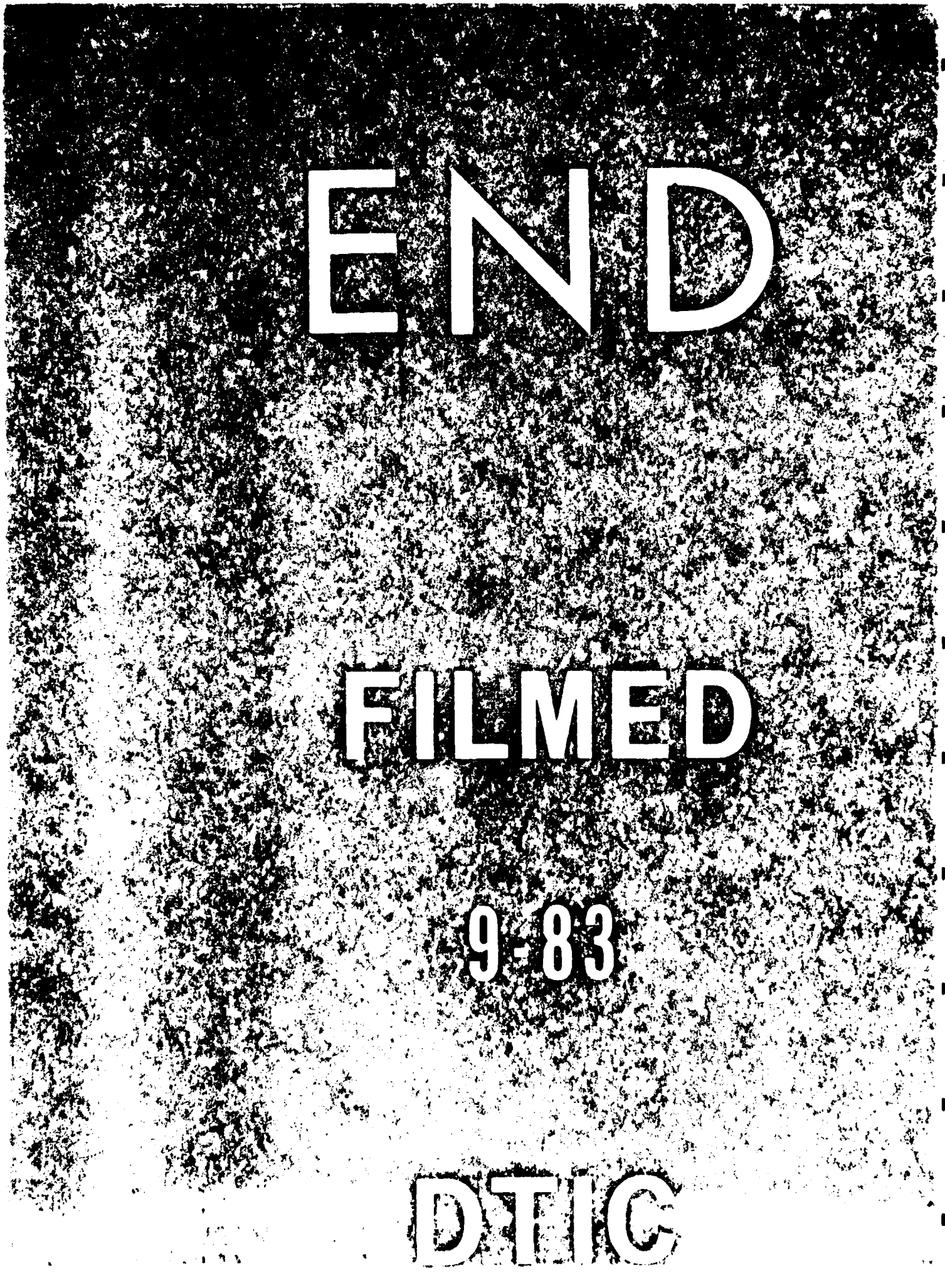
END
FILMED
9-83
DTIC